A study on the effect of mortar joint strength and placement on masonry blockwork wall capacity.

Nick Xuereb

Dissertation submitted to the

Faculty for the Built Environment, University of Malta

In part fulfilment of the requirements

for the attainment of the degree

Master of Engineering (Structural Engineering)

June 2025

L-Università ta' Malta

FACULTY/INSTITUTE/CENTRE/SCHOOL_FOR THE BUILT ENVIRONMENT__

DECLARATIONS BY POSTGRADUATE STUDENTS

(a) Authenticity of Dissertation

I hereby declare that I am the legitimate author of this Dissertation and that it is my original work.

No portion of this work has been submitted in support of an application for another degree or qualification of this or any other university or institution of higher education.

I hold the University of Malta harmless against any third party claims with regard to copyright violation, breach of confidentiality, defamation and any other third party right infringement.

(b) Research Code of Practice and Ethics Review Procedures

I declare that I have abided by the University's Research Ethics Review Procedures. Research Ethics & Data Protection form code ______BEN-2024-00119______.

As a Master's student, as per Regulation 77 of the General Regulations for University Postgraduate Awards 2021, I accept that should my dissertation be awarded a Grade A, it will be made publicly available on the University of Malta Institutional Repository.

02.2023

Acknowledgements

I would like to thank my tutor Prof. Spiridione Buhagiar B.E.&A. (Hons),M.Sc.(Lond.),D.I.C.,Ph.D.(Lond),F.I.Struct.E.,M.S.C.E.,Eng.,Perit for all his expertise, advice and constant guidance throughout the entire duration of writing this dissertation and the six years I spent at this faculty.

I would like to further extend my gratitude to Nicholas Azzopardi and Alex Falzon for their constant aid and guidance throughout the entire testing process at the laboratory. As well as the entire Faculty for the Built Environment, for their constant dedication to improving our trade.

I could not have done any of this without the constant support of my family and friends, as they encouraged me throughout this entire process. Lastly, I extend my heartfelt gratitude to UM Wolves RFC for their unwavering support as the university's rugby club, which has been invaluable throughout my academic journey.

I take full responsibility for any shortcomings in this dissertation.

Abstract

In the past decades there has been a boom in construction on the Maltese Islands. This has led to multiple cases of poor workmanship in local projects. Masonry walls are key components in construction; however, an aspect that is often overlooked locally is the mortar joint, relying more on the brick for structural strength. In both the local MSA annex of Eurocode 6 and international versions of Eurocode 6 it is specified that both the blocks and the mortar used have to be specified to accommodate certain standards. While masonry units are covered under standards such as EN 771-5:2011 and more specifically EN 771-3:2011 for aggregate concrete masonry units, this dissertation focuses more on the mortar. The mortar to be used with masonry similarly has to conform to EN 998-2, which outlines relevant tests such as EN 1015-11 for compressive strength, among other standards such as EN 1052-2 and EN 1015-3 which address mortar properties.

However, the effects of mortar placement and workmanship remain under-investigated in the local context, with only brief mentions in Eurocode 6. Mortar placement influences not only the compressive strength of a wall but also its overall performance , including water penetration, shear resistance, flexural strength and insulative characteristics. Hence the identification of the effects of laying of mortar in masonry walls within construction is of interest. The variation of mortars (general-purpose, lime based, cement based etc) have been well standardised in EN 1015:1999, however, different mortar types impact the strength and composite behaviour of the masonry wall differently, making this the key parameter of the investigation. Locally speaking for Hollow Concrete Blocks (HCB) typically, a 1:3: cement to sand ratio is used according to the local licensed mason’s handbook. That being said the national annex specifies mortar based on its strength. For concrete units, a general-purpose mortar of strength M2, M6, M10 or M20 is to be used.

Keywords

Masonry, Mortar, Compressive Strength, Structural Behaviour.

Table of Contents

List of Figures

List of Tables

1. Introduction

1.1 Aims and Objectives

The placement of mortar in masonry block construction affects not only the compressive strength of the wall but also its overall properties, including water penetration, shear resistance, flexural strength, and thermal insulation. Another aspect that determines the structural behaviour of a masonry wall is the variation in mortar type in mixes, such as general-purpose, lime-based, and cement-based mortars, which have been well-standardised in EN 1015:1999. Each type of mortar has different mechanical properties, including elastic modulus and compressive strength, which directly influences the strength of the joint and the overall strength and deformation behaviour of the masonry wall. Local construction practices predominantly use guidelines for mortar mixes based on the licensed mason's handbook. For hollow concrete blocks (HCB), this handbook recommends a 1:3 cement-to-sand ratio (Camilleri, 2023). This is in contrast to other European countries, such as France, which use ready-mix mortars instead of mixing the base components on-site (MCT Italy, n.d.). This study aims to establish the effects of mortar placement strength on masonry walls made of hollow concrete blocks (HCB) using wallette construction through experimentation and comparison of results by varying mortar placement and joint strength.

1.2 Research Questions

The following research questions require clarification:

- *What are the effects of poor workmanship concerning mortar placement in masonry wall construction?*
- *What are the effects of mortar strength on masonry wall construction?*
- *What are the failure modes that occur due to different joint characteristics?*
- *What are the effects of mortar placement on the load paths within the block?*

1.3 Research Justification

Over the past few decades, there has been a boom in construction on the Maltese Islands (NSO, 2021). This has resulted in multiple instances of subpar workmanship, as seen in **Figure 1.1.** Masonry walls are key components in construction; however, an aspect that is often overlooked is the mortar joint, which relies more on the brick for structural strength. The effects of mortar placement have not been studied extensively within the local context, with only brief mentions in Eurocode 6 discussing shell bedding. Hence, the identification of the effects of mortar placement in masonry construction is of interest. In order to further understand the effects of poor workmanship on load bearing walls and the structural behaviour of mortar and masonry.

Figure 1.1: Examples of poor workmanship, Marsaskala, Malta

1.4 Research Method

The research will be conducted through experimentation, during which quantitative data will be collected. The main apparatus being used will be; (a) Load Cell; having a capability of recording loads up to 1000kN (b) No.2 ; LVDT – Linear Variable Differential Transformer. Two 50 mm LVDTs will be used to measure vertical displacement, which will be placed on top of the spreader beam. The LVDTs are being placed on top of the beam to avoid any damages occurring during testing.

As seen in **Figure 1.2a**, the tests will be carried out on wallettes constructed from three hollow concrete blocks via compression with various test setups. Ideally, these tests would have been conducted multiple times to determine a statistical mean; however, it was preferred to vary one component at a time as an exploratory study such as joint material, curing time, and placement, as seen in **Figure 1.2 b**. This is done to understand the flexure, strength, and load path of the Hollow Concrete Block and its relation to mortar placement, stiffness, and strength. In addition to using different materials instead of mortar at the joint, in order to create a comparison.

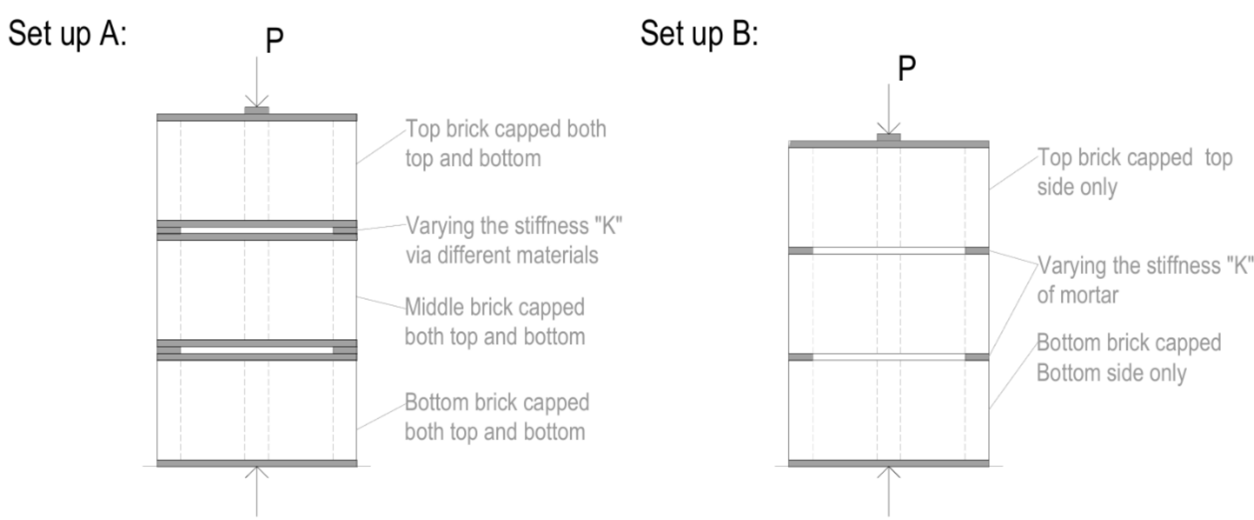

Figure 1.2a: Test set ups for Wallettes

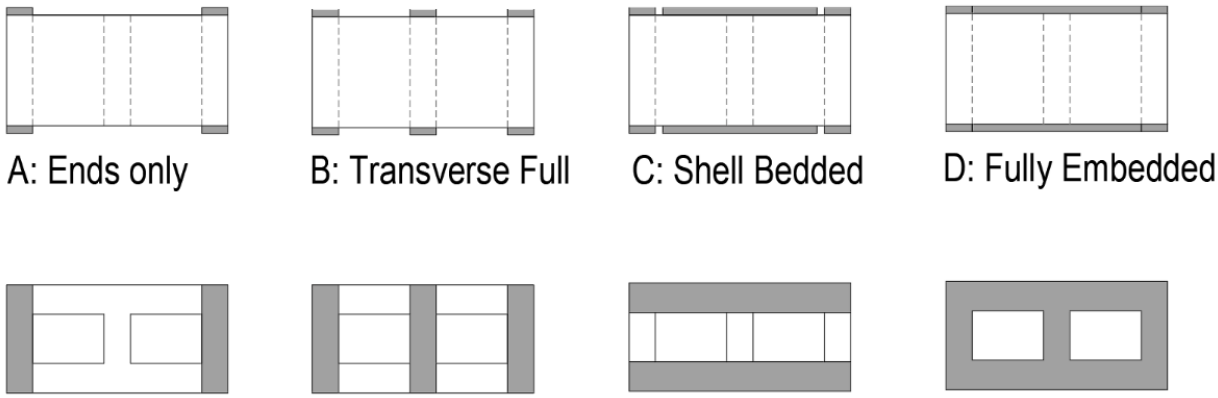

Figure 1.2b: Variation of Joint Placement

The control for the wallette tests is a single compressive test on the hollow concrete block, which is double capped, serving as the basis for the wallettes strength, as shown in **Figure 1.3**. The mortar prisms are also tested to obtain a value for strength. The results are then plotted as stress-strain curves from the logged results of load and displacement. Taking the same gross area throughout, as opposed to the net area, and measuring the height of each wallette. For comparison, the hardest joint is that of steel, and the softest is neoprene; hence, mortar lies somewhere in between in terms of pure strength, as seen in **Figure 1.4.** Approximately 70 units of 230 mm “tad-disa”, ” dobblu” (Double density) bricks are to be used.

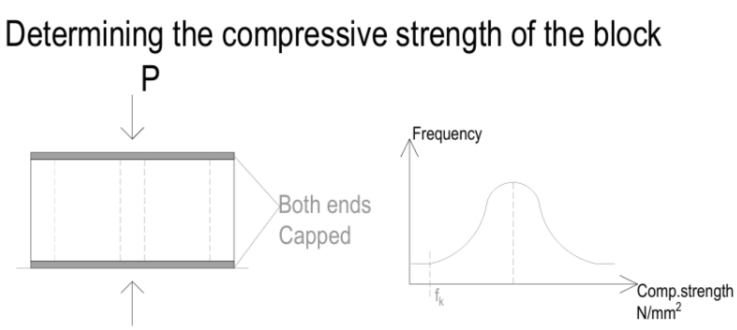

Figure 1.3: Control Test

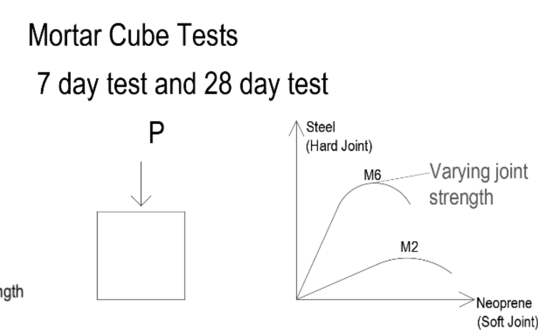

Figure 1.4: Mortar Testing

1.5 Dissertation Structure

Chapter 2 – Literature Review

A literature review gives a theoretical basis to a dissertation. Hence, the second chapter reviews the literature read to provide a solid background and context for the research being conducted. It introduces the material and research studied and then discusses the application and importance of this dissertation. The review examines standards for masonry and mortar construction, as well as related research. It also outlines the research gaps present and what potential further research could be done in this dissertation or other research. It also outlines the current limitations of standards and research present. Keeping in mind that the literature is to be relevant to the related research questions and to be critically analysed.

Chapter 3 – Methodology

This chapter describes the research process, including the testing procedures, as well as the limitations and difficulties encountered during sample preparation and testing. This includes the specification of a rig setup, materials, and specimens.

Chapter 4 – Results and Discussion

This chapter exhibits and tabulates the results obtained, as well as an interpretation of these results, accompanied by graphs and tables for a better understanding of the structural behaviour being investigated. Alongside the results, there is a discussion regarding previous literature and analysis derived from the experimental investigation results. Generally, the results demonstrate the strength of the mortar and wallette, as well as the strain obtained through testing.

Chapter 5 – Conclusion

The final chapter concludes the dissertation with closing remarks, as well as a description of the limitations within the process and potential improvements made, along with suggestions for further research.

2. Literature Review

2.1 Introduction

This chapter reviews the relevant literature surrounding the structural behaviour of masonry, with a particular focus on the composite behaviour between mortar and block units. It examines the influences of compressive strength through mortar mix design, unit properties, joint configuration and workmanship. As well as, looking into the properties of mortar such as moisture content, aggregate characteristics and environmental factors. Multiple studies were discussed to highlight and look into the complex relationship between block units and mortar, to be a reference for the tests carried out within the methodology of this dissertation. By getting a broad amount of research locally and internationally, this review aimed to identify research gaps that are relevant to unreinforced hollow concrete blockwork under axial compression with respect to its behaviour to mortar joints.

Furthermore, in both the local MSA annex of Eurocode 6 (MSA EN 1996-3:2006) and international versions of Eurocode 6 it is specified that both the blocks and mortar used must conform to recognised standards. This standardisation aligns with local obligations as an EU member state, whereby construction materials, including masonry units, are required to bear the “CE” mark in accordance with harmonised European standards such as as EN 771-5:2011, which outlines the relevant performance characteristics of masonry units and more specifically, BS EN771-3:2011 for aggregate concrete units.

The mortar used with masonry must similarly conform to EN 998-2:2016; within the standard it outlines tests to be followed such as EN 1015-11:1999 for compressive strength, among other standards that deals with testing of mortar, such as EN 1052-2:1999 and EN 1015-3:1999 which deals with mortar properties, which are referenced within Eurocode 6 (EN 1996-1-1:2005). Furthermore, the national annexe specifies mortar based on its strength. For concrete units, a general-purpose mortar of strength M2.5, M5, M10, or M20 is to be used (MSA EN 1996-3:2006). It is important to note that in EN 1052-1:1999 the compressive strength of masonry is derived from tests using uniformly applied loads and not point loads hence it does not cover this area, and it is a limitation of the standards present.

2.2 Compressive Strength of Masonry Construction

Three conditions affect masonry compressive strength.

(i) Mortar mix strength, such as M2, M6 and non-standardised mixes. The sand-cement ratio determines the properties of the mix (EN 1996-1-1:2005). As well as the water content affects the mix properties (Haach et al, 2011) but this is not prescribed by the standard. Instead, the standard (BS EN 998-2-2016) leaves it up to the user to find their needed workability.

(ii) Properties of Block units, directly affect the strength of masonry units. Primarily compressive strength, unit type (clay, calcium silicate, concrete, autoclaved aerated concrete, stone) and geometry (size, hole volume, orientation) which influence their structural behaviour (EN 1996-1-1:2005).

(iii) Site Conditions and Workmanship, this is recognised in the standard and good practice is recommended (EN 1996-1-1:2005). However, it is not directly accounted for in calculations, but rather indirectly addressed through the use of material partial safety factors in design.

Mortar is not only used to bed blocks but also used to maintain the course height. Testing shows that the bulk densities of the mortars have a direct effect on the deformation and compressive strength of the mortar. (Haach et al , 2011).

$$\mathbf{f_k = K\, f_b^{\alpha}\, f_m^{\beta}} \qquad \textbf{(equation 3.1 of Eurocode 6, Part 1-1)}$$

$$\mathbf{f_k = K\, f_b^{0.7}\, f_m^{0.3}} \qquad \textbf{(equation 3.2 of Eurocode 6, Part 1-1)}$$

$$\mathbf{f_k = K\, f_b^{0.85}} \qquad \textbf{(equation 3.3 of Eurocode 6, Part 1-1)}$$

$$\mathbf{f_k = K\, f_b^{0.7}} \qquad \textbf{(equation 3.4 of Eurocode 6, Part 1-1)}$$

Figure 2.1 : Equations from Eurocode 6, Clause 3.6.1.2, EN1996-1-1(2005)

Note:

- *Equation 3.2 refers to general purpose mortar and lightweight mortar*
- *Equation 3.3 refers to thin layer mortar with bed joint thickness of 0.5 – 3 mm f_m is ignored, for groups 1 and 4.*
- *Equation 3.4 refers to thin layer mortar with bed joint thickness of 0.5 – 3 mm f_m is ignored, for groups 2 and 3*

Mortar and Block strength together make up the compressive strength of the wall. According to EN 1996-1-1:2005, clause 3.6.1.2, that f_k the characteristic compressive strength of the masonry system, is used to describe the compressive strength of the wall construction in N/mm^2(MPa). It is specified that when perpendicular joints are unfilled, equation 3.1 of EN1996-1-1:2005, as seen in **Figure 2.1** may be used with consideration of any horizontal actions that are applied to the masonry. In which the mortar type (general purpose mortar, thin layer mortar, lightweight mortar) affects the value of K, as well as the values of α and β used. To obtain the design compressive strength f_d a material safety factor must be applied to f_k.

However, no mention is made of parallel joints i.e. bed joints not being filled. There is limited direct research or prescriptive guidance on the effects of this in Eurocode 6 (EN 1996-1-1:2005) and relating standards, suggesting that this is not a common practice in masonry construction. As in the code, full embedment of the bed joint is recommended as it is essential for structural integrity and durability of the masonry wall (EN 1996-1-1:2005). However, from a base structural mechanics perspective, unfilled bed joints would significantly reduce load transfer due to increased load transfer and stress distribution.

EN 1996-1-1:2005 mentions partially filled joints, i.e., shell-bedded masonry being only partially filled via two strips of mortar longitudinally. Shell bedding reduces the compressive strength of masonry but also allows for rain penetration (Roberts & Brooker, 2007). One should also note that there may be a local failure due to it not being filled throughout; hence, this must be checked. Note that equation 3.1 as seen in **Figure 2.1** does not refer to shell bedded masonry, it instead has to be altered to account for this strength reduction by modifying the factor K. (Roberts & Brooker, 2007).

Equation 3.1 in **Figure 2.1** is based on tests in accordance with BS EN 1052-1:1991. This is a standard that deals with methods for determining the compressive strength of masonry perpendicular to the bed joints. It defines the preparation of specimens, conditioning prior to tests, the equipment used, methodology and contents of the final report. The test specimens are loaded uniformly until they fail via crushing. It does not take into consideration the effects of loading restraint, slenderness or eccentricity due to the set up specified by the standard testing being for axial uniform compression. The conditions of the units should be known such as age, moisture content and weight, for comparison of data. (BS EN 1052-1:1991)

BS EN 1052-1:1991 then recommends the use of BS EN 772–1:2011 for lab testing. This standard outlines the process by which masonry units are prepared for compressive strength testing. It discusses how to cap the masonry with mortar, taking into account different conditions, such as voids similar to a hollow concrete block or when one is to be shell bedded. It also discusses air-dried vs. oven-dried conditions as multipliers are applied on the compressive strength based on moisture content, for example 1 for air dried whilst 0.8 for oven dried specimens (BS EN 772-1:2011). During testing, the loading is uniform to ensure uniform displacements across the loaded surface. (BS EN 1052-1:1991).

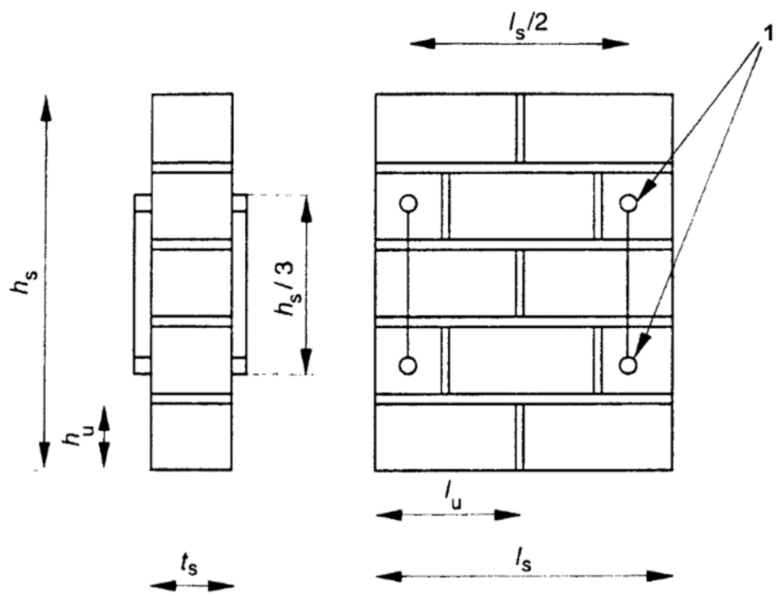

Figure 2.2: Recommended Masonry Specimen in Testing BS EN 1052-1:1991

2.2.1 Axial Loading of Masonry

Buhagiar, (1985) states that in failure due to axial loading, a masonry block unit will experience a vertical splitting due to horizontal tension forces. It is also observed that masonry walls, as a whole, have less compressive strength compared to the individual units when tested. Hence, one cannot take the characteristic compressive value for the strength of a single unit and apply it to a wall in a linear manner, as this is not representative of the actual behaviour of a masonry structure. The failure of a wall is dependent on both the structure itself and the mortar joints, as they are a composite element. During compression, the joints expand, which puts a tensile stress on the blocks. If it is acting as a shear wall, the lateral movement is resisted by the perpendicular mortar joint between the masonry. Hence, at the ultimate compressive strength of the block, there will be a failure due to tensile stress. (Buhagiar, 1985).

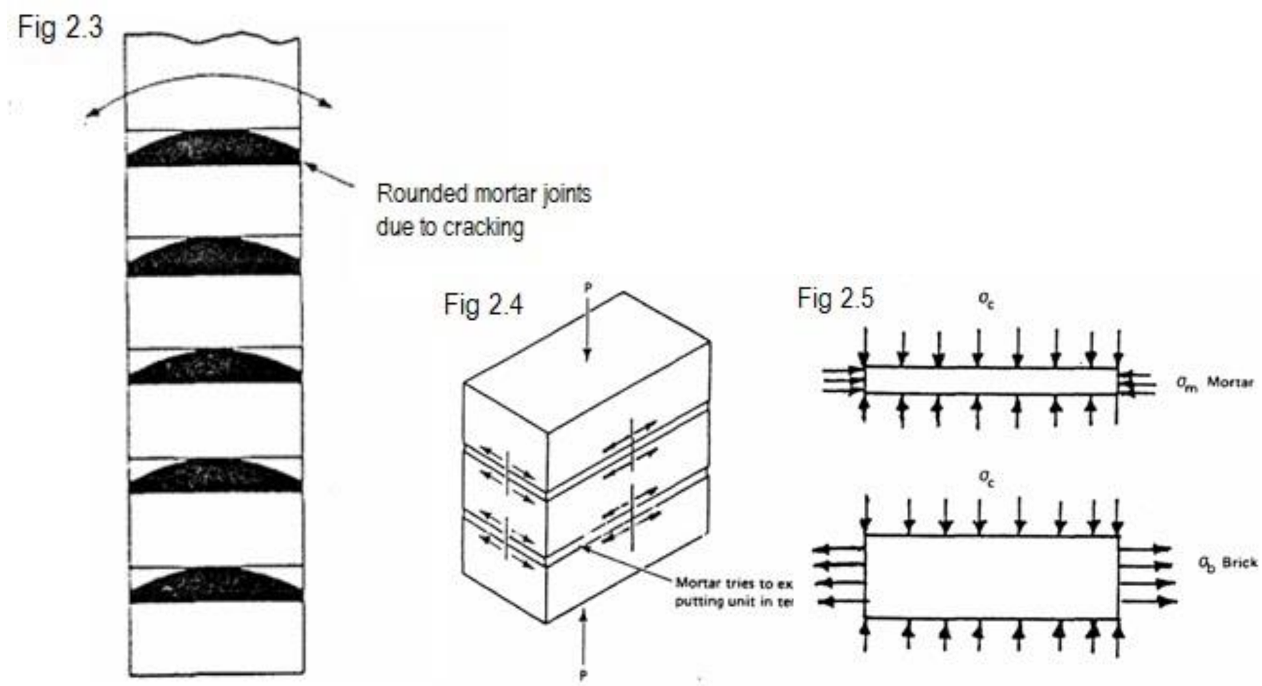

Figure2.3: Rounded Mortar joints, (Buhagiar, 1985, page 11/180)

Figure 2.4: Mortar Bed Compression (Buhagiar, 1985, page 11/180)

Figure 2.5: Elastic Theory of Masonry Failure (Buhagiar, 1985, page 11/180)

2.3 Bonding Capacity of Mortar

It is a common assumption that mortar has little bonding capacity, however in reality, mortar transfers axial compressive stress from one block to another Bartolo et al , 1991). The degree of how much axial stress is transferred and the effects of placement are unknown and are recognised to be a research gap that this research aims to investigate.

Bartolo et al , (1991) states that another consideration in terms of analysis is whether the mortar is acting plastically or elastically. Once crushed the mortar can be assumed to be acting plastically, with the original mortar being in the elastic condition.

One should also note that there is a physical relationship between the bonding of masonry blocks within itself i.e. the overlap of the blocks. EN1996-1-1: 2005 recommends the following:

(1) Masonry units when unreinforced should be overlapped at alternate courses so the wall acts as a single element.

(2) The length of walls and size of openings as well as piers should be coordinated with block dimensions to avoid excessive cutting.

(3) If the wall is reinforced the minimum bonding arrangements may be overlooked given appropriate experimental data or experience deems it satisfactory. Hence the degree of overlap is determined as a part of the design.

(4) For mortar joints, it is recommended that the actual thickness of both bed joints and perpendicular joints should not be less than 6mm and not more than 15mm thick for general-purpose and lightweight mortars. Exceptions are made between 3mm and 6mm if designed specifically for said thickness for general purpose mortars, as is the case in this dissertation as **5mm** joints were used. For thin layer mortars, an actual thickness of not less than 0.5 mm and not more than 3 mm is recommended.

(5) The minimum overlap is shown in the following figure: (EN 1996-1-1, 2005)

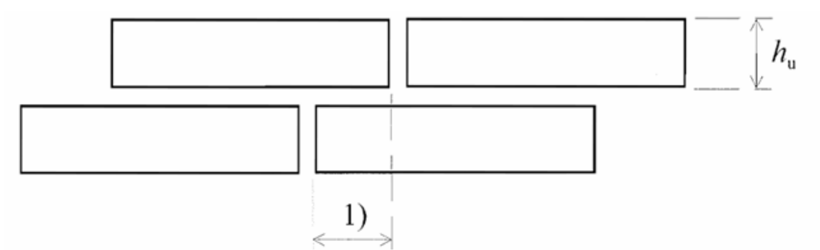

$$1)\quad \text{overlap}\begin{cases}\text{when } h_u \leq 250\text{ mm : overlap} \geq 0{,}4\ h_u \text{ or 40 mm, whichever is the greater}\\ \text{when } h_u > 250\text{ mm : overlap} \geq 0{,}2\ h_u \text{ or 100 mm, whichever is the greater}\end{cases}$$

Figure 2.6: Overlap of Masonry Units (EN 1996-1-1, 2005)

2.4 Mix Properties of Masonry and Mortar

Mix design of mortar has a critical role in the overall behaviour and strength of masonry units. This section will look into how the different factors such as moisture content, aggregate fines, environmental conditions and workability affect the performance of masonry. These variables are relevant to this dissertation and local practice, due to common materials used such as "Xaħx" and Hollow Concrete Blocks, under variable environmental conditions. By reviewing available research this section investigates the mechanical properties of mortar and its effects on masonry performance. This gives context for the experimental research carried out in this dissertation.

2.4.1 Moisture Content

Clause 5.2 of BS 5628-3:2001 discusses masonry, materials, component design as well as workmanship with respect to stability. Clause 5.4 of BS 5628-3:2001 further discusses movement in masonry due to changes in (a) temperature (b) moisture content (c) water vapour. This is relevant as , locally , as we use highly porous blocks such as limestone or more porous hollow concrete blocks (HCB), which absorb moisture rapidly within such a dry humid environment. Furthermore, it can be said that during the curing period when initially being laid, such a high rate of absorption can be detrimental to the bond between mortar and masonry. Moisture significantly affects the strength characteristics of mortar as demonstrated by Haach et al (2011) through 28-day hardened mortar tests, showing that if cured too quickly this causes a reduction in compressive strength. This indicating that water retention is crucial for strength gain in mortar.

2.4.2 Aggregates Fines Content

Bartolo et al, (1991) demonstrate that the amount of fines in a mix affects the air content and void ratio of the mortar. This is critical when using "Xaħx" as it contains a high level of fines. Hence, more air-entraining agents may be needed for the same air content. Prior to the addition of cement, the aggregate absorbs more water; this increases the total water demand. Haach et al (2011) also show that fine aggregates raise water demand and influence compressive strength. Hence when using a large amount of fines, the mix may be denser and stronger; however, if too much water is used for workability this may be reduced. One should also note that "Xaħx" is a by-product of cutting stone; hence, it comes from a weak parent material, globigerina limestone.

Hence, some masons pre-wet the units to reduce the effects of highly absorbing units, avoiding high initial hydration of the mortar (Bartolo et al , 1991).

2.4.3 Environmental conditions

Locally we tend to get very high temperatures as well as strong winds at times which make the mortar dry quickly. Hence why it is good practice to wet masonry on both top and bottom surfaces (Camilleri 2023), however generally this is difficult due to practicality of rotating the brick and doing the bottom side as well as time constraints on site. The control of environmental conditions is difficult on site with the primary main consistent variable being relative high humidity locally (NSO 2022). If the mortar is too wet, it may cause bleeding and segregation of the mix, reducing cohesion and making it weaker due to losing parts of its cement binder. (Haach et al, 2011)

2.4.4 Workability

Workability is a key consideration in workmanship when constructing masonry walls and therefore it dictates the chosen mix proportions. This is generally controlled by the water-cement ratio. In which excess water increases fluidity but may cause bleeding and segregation hence reducing adhesion and cohesive properties of the mortar. Haach et al, (2011) also show that workability is not solely dependent on water content but also by the grading and particle size distribution of the aggregates. Well graded mortars in the study demonstrated better cohesion with lower void ratios and better compressive hardened performance.

2.4.5 Mix Consistency

Bartolo et al , (1991) observed that when comparing wet and dry mixes, they lost air at a similar rate over time. As a result, it is clear that, that the loss of air entrainment is not directly influenced by the water content in the fresh mix. Nor does sand, however the size of the sand particles does influence the amount of air trapped in the mix. It was shown that coarser sands retain more air than finer sands. It was concluded that the chemical reaction associated with cement hydration is what caused air loss. One should note that there is a distinct difference between Xaħx and sand. Sand is a by-product of crushing whilst Xaħx is a by-product of chipping limestone and quarry dust.

2.5 Lateral Resistance of Mortar

Lateral load analysis of walls is essential due to varying lateral loads such as wind, retainment, seismic and eccentric axial loads which cause masonry to act as shear walls. A common case of both a wall taking lateral and vertical loading would be a basement wall acting as a retaining wall. The lateral capacity of a wall depends on the shear strength of the joint, tensile bond and flexural bond strength. The adhesion of mortar is also a contributory factor however, when considering lateral actions or combined bi-axial moments in pure axial compression, it is not as relevant. Eurocode 6 emphasizes tensile bond strength as crucial for flexural resistance in laterally loaded wall panels (Roberts & Brooker, 2007). In testing a traditional Limestone wall, Bartolo et al (1991) noted that when joints fail, they would crack along the mortar joints resulting in a restricted load path, therefore increasing the build-up of stresses on the part of the wall which is still in contact. Whilst when testing an unreinforced Hollow Concrete Block wall, Yancey et al (1991) noted that failure often initiates at the bed joints where diagonal shear cracks develop, progressively reducing the wall's load-bearing capacity. These cracks propagating along the mortar joints interrupting the original load path, causing stress concentrations. Such joint-driven diagonal cracking is a common failure mechanism in unreinforced HCB shear walls.

For design of lateral resistance of a masonry wall with abutting units and unfilled perpendicular joints, the code provides this equation for shear strength: $\mathbf{f_{vk} = 0.5\ f_{vko} + 0.4\ \sigma_d \leq 0.045\ f_b}$ **Eurocode 6, EN 1996-1-1:2005, Clause 3.6.2**

Where f_{vk} is the characteristic shear strength of masonry, f_{vko} is the initial shear strength, σ_d is the design compressive stress, f_b is the compressive strength of the block unit.

Hence unfilled joints reduce both the compressive strength of a wall as well as the flexural lateral strength (Roberts & Brooker, 2007). In the national Maltese annex of EC 6 (MSA), a more detailed approach is provided to find the design shear resistance of a shear wall is found by taking it as a rectangular section and finding the design shear stress V_{Rd} :

$$V_{Rd} = c_v[0.5-e_{Ed}]tf_{vdo}+0.4(N_{Ed}/\gamma_M) \leq 3[0.5-e_{Ed}]tf_{vdo}$$

MSA EN 1996-3:2006,Cl. 4.4.2 Where V_{Rd} is the Design Shear Resistance, c_v is the coefficient for joint conditions, e_{Ed} is the eccentricity, t is the thickness , f_{vdo} is the design value of the initial shear strength, N_{Ed} is the axial load.

It can be further said that shear resistance is influenced by both the bond shear strength of the joint as well as the frictional resistance at the block-mortar interface. (Bartolo et al, 1991)

2.6 Influence of Joint Properties on Masonry

The performance of masonry walls is directly influenced by the characteristics of its joints, such as thickness, strength, configuration and embedment. Mortar joints do not only act as bonding elements but play a key role in load transfer, stiffness and failure mode of the entire masonry wall. Hence understanding variations in said properties and how they affect structural performance is critical, especially in unreinforced systems such as hollow concrete block (HCB) walls. This section reviews and analyses experimental studies both local and international, that investigate the effects of such characteristics. This was done to give context to joint behaviour with respect to the experimental methodology of this dissertation.

2.6.1 Influence of Joint Thickness on Masonry

As masonry structures are composite elements, it is important to understand the effects of mortar joint thickness as it ensures load transfer in the overall element. Caldeira et al, (2020) researched to observe the effects of mortar joint thickness on the compressive behaviour of wallettes made of hollow concrete blocks (HCB). The mortar joint thickness was varied from 5, 10, 15, 20 mm. This is relevant as in the methodology proposed for this dissertation the joint strength is to be varied hence such variations will affect the results. In said study, 120 prism units made of two bricks with dimensions were used 390 x 137 x 188 mm (Caldeira et al, 2020). This differs from the three 230mm block prisms to be used in this dissertation; however, it is still similar enough to be a valid comparison in terms of testing.

Figure 2.7 illustrates the various failure scenarios generated by varying the mortar thickness and strength. For example, in scenario "A", a 20mm mortar joint was used with a strength less than 40% of the block used, and hence failed due to mortar crushing, resulting from a weak mortar. In Scenario "B" , transverse block splitting was experienced due to having a stronger mortar but still not exceeding the block's strength. Whilst in scenario "C" the mortar exceeded the block's strength and experienced block crushing. (Caldeira et al, 2020)

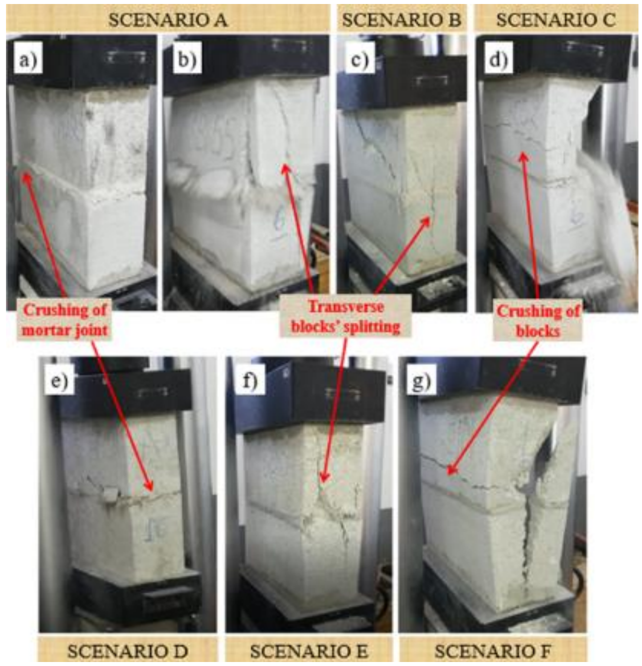

Figure 2.7 : Failure Modes (Caldeira et al, 2020)

Caldeira et al, (2020) observed that the results of the tests indicate that joint thickness is inversely proportional to the compressive strength and stiffness of the masonry prisms. Hence, a thinner joint, such as the 5 mm joint used, performed better than the 20 mm joint used. In theory, the ideal situation is one of isotropy, with no variation in mortar thickness or strength. This highlights the importance of proper and consistent workmanship on-site when it comes to masonry wall construction.

It should be noted that a previous dissertation at the University of Malta studied the effects of joint thickness with respect to globigerina limestone masonry wall strength. The research's aim was to vary the mortar thickness on traditional masonry globigerina limestone wallettes, with three units stacked on top of each other, to see the effects on strength. The variation in mortar thickness ranged from 5mm to 15mm in the fully embedded condition. The findings suggest that beyond a 5mm thickness, there may be an increase in axial capacity. This contradicts common notions that thinner mortar joints are stronger for masonry strength, as seen by the thickness limits set by Eurocode 6 (Roberts & Brooker, 2007). In this case, it was stated that the highest strength was obtained at a 10mm thickness (Caruana, 2024). This suggests that the relationship between mortar thickness and masonry strength is not purely inversely proportional, but rather more complex.

2.6.2 Influence of Joint Strength on Masonry

Fonseca et al. (2017) conducted experimental research to investigate how mortar strength affects the failure mode and ultimate compressive strength of HCB Prisms, using three blocks stacked on top of each other. This research showed that the mechanical behaviour and failure mechanism of masonry is fundamentally controlled by the mortar's properties as opposed to the block's properties alone. The testing methodology involved testing stack-bonded prisms all constructed from the same type of hollow concrete block with three types of mortar, the variation being the mortar strength. The type 1 mortar has a mean of 20.3 MPa. The type 2 mortar has a mean of 7.4 MPa, and the type 3 mortar has a mean of 4.5 MPa. It should be noted that each prism type was tested at least three times for a mean statistical value. The results from the testing showed that, although the compressive strength of the masonry increased with stronger mortars, the most critical factor was the change in failure modes depending on the relative strength of the mortar to the block, which had a mean strength of 23.1 MPa. This indicates that overall, the unit strength tends to dictate the compressive capacity of masonry, while mortar properties influence failure mode and strain response.

For the strong mortar type, the masonry behaved like a homogeneous material, with failure induced by tensile cracking in the blocks that propagated through the mortar joints. This demonstrated that the reaction of the prism was uniform under the specified load. This is in contrast to weaker mortars in which localised crushing in the mortar caused stress concentrations and cracking in adjacent blocks. It is important to note that, even in the case of weak mortar, a considerable amount of the block's capacity was reached, showing that block strength alone does not reveal the factors leading to failure. The research highlighted that non-linear stress-strain behaviour is central in evaluating the performance of masonry. The weak mortar prisms exhibited bilinear stress-strain curves, with nonlinearity occurring early, prior to the ultimate load, as seen in **Figure 2.8.** This early transition indicates internal cracking or pore collapse within the mortar joint, which would go unnoticed if only ultimate strength is noted. This is in contrast to the strong mortar prisms, which maintained linearity relatively until failure, indicating a sudden, more brittle failure mode, as seen in **Figure 2.9.**

A key finding from Fonseca et al (2017) is that, in most design codes, the primary factor in compressive strength primarily relies on the block's strength, which may not accurately represent the failure mode, especially in weaker mortars. Hence, their research promotes the incorporation of non-linear behaviour and mortar contribution into predictive models of masonry strength. This emphasises the consideration of accurate stiffness degradation and deformation characteristics for safer masonry design. Hence, it highlights the importance of evaluating the stress-strain response with respect to the structural performance of masonry walls, which is dictated by the mechanical behaviour and failure mechanisms of mortar strength. (Fonseca et al, 2017)

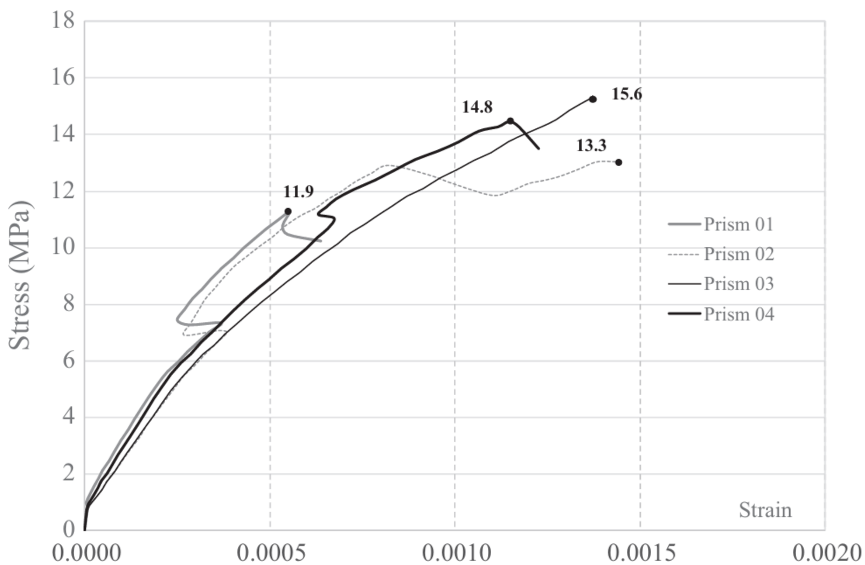

Figure 2.8 : Stress-Strain Relationship for four masonry prisms built with mortar III

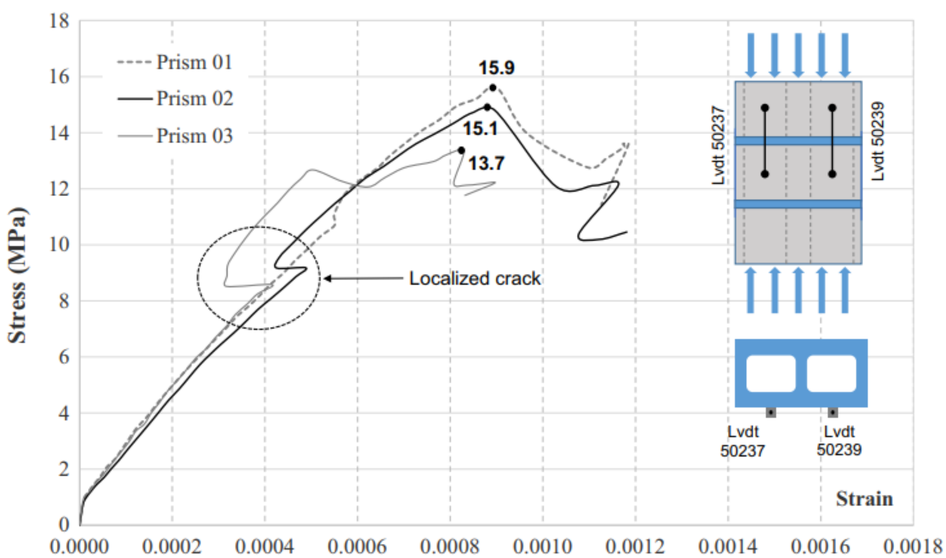

Figure 2.9 : Stress-Strain Relationship for three masonry prisms built with mortar I

(Fonseca et al, 2017)

In another study by Sarhat et al. (2014), an experimental investigation was conducted into the compressive strength of ungrouted (no filled cavities) hollow concrete masonry prisms. In the said research, 248 data sets were reviewed, comprising 1092 individual prism test results. The primary objective of the study was to establish a reliable predictive model for compressive strength based on the strength of the masonry unit, mortar strength, bedding, and the height-to-thickness ratio of the prism. Based on these results, the researchers developed a multiple-power regression model that accounted for 82% of the variance in the collected test data, which was an improvement over traditional $f'_{\mathrm{m}} = 1.107(f_{\mathrm{bl}})^{0.750}(f_{\mathrm{mr}})^{0.180}$ code-based prediction models. **Equation (1) from Text (Sarhat et al, 2014)**

The main findings showed that both block strength and mortar strength correlated with overall masonry compressive strength, with block strength being more consistent compared to mortar, which was more scattered. In this study, full embedment was compared to shell embedment, considering their relative areas. Consequently, the shell bedded case yielded a higher compressive strength based on the face shell area rather than the net area. This went against what international codes, such as EN 1996-1-1:2005, stipulate. (Sarhat et al , 2014). It should be noted that EN 1996-1-1:2005 uses gross area as opposed to the actual area.

2.6.3 Influence of Joint Configuration and Failure Mode via Head Joints

In a previous study by Fonseca et al. (2015), the influence of joint configuration was examined, particularly the addition of head joints. The head joint being the vertical mortar joint between two adjacent masonry units. This was done by initially setting up a prism with 3 blocks on top of each other, as opposed to a larger wall set up with 2 blocks and a half block for a single coarse, with a total of 5 courses, as seen in **Figure 2.10.** This allowed for further examination of the deformation and failure behaviour of hollow concrete masonry, not just through the mortar joint but also through variability in prism configuration. This variation created a weaker point in the load path, resulting in a reduction in compressive performance and altering the failure mode due to the head joint.

Two mortar types were used , a strong 18.2 MPa type 1 mortar which saw a reduction in 42% and a weak 8.30 MPa type 2 mortar which saw a reduction in 66% in terms of compressive strength, in comparison to a full prism. Note that the hollow concrete blocks used had a strength of 23.1 MPa. As the 3 block prisms are simpler, in comparison the head joint caused an increase in the coefficient of variation in the results due to variance in bond strength at said interfaces. This emphasises the importance of joint placement and workmanship in bond strength at the interface as non-uniformity in the joint can cause localised failure paths. (Fonseca et al, 2015)

In terms of failure mode, the prisms with bed joints had clean vertical cracking and brittle failure particularly with stronger mortars. This is in contrast to prisms with head joints which exhibited more complicated failure modes, such as cracks initiating at the joint, causing progressive crushing of mortar, which led to prism face spalling and scattered cracking. The difference in failure mode due to crack propagation indicated the influence joint configuration has in ductility and predicted masonry failure. The advantage of this study was that it more accurately resembled full wall elements. (Fonseca et al, 2015). Note; the term prism and wallette are interchangeable.

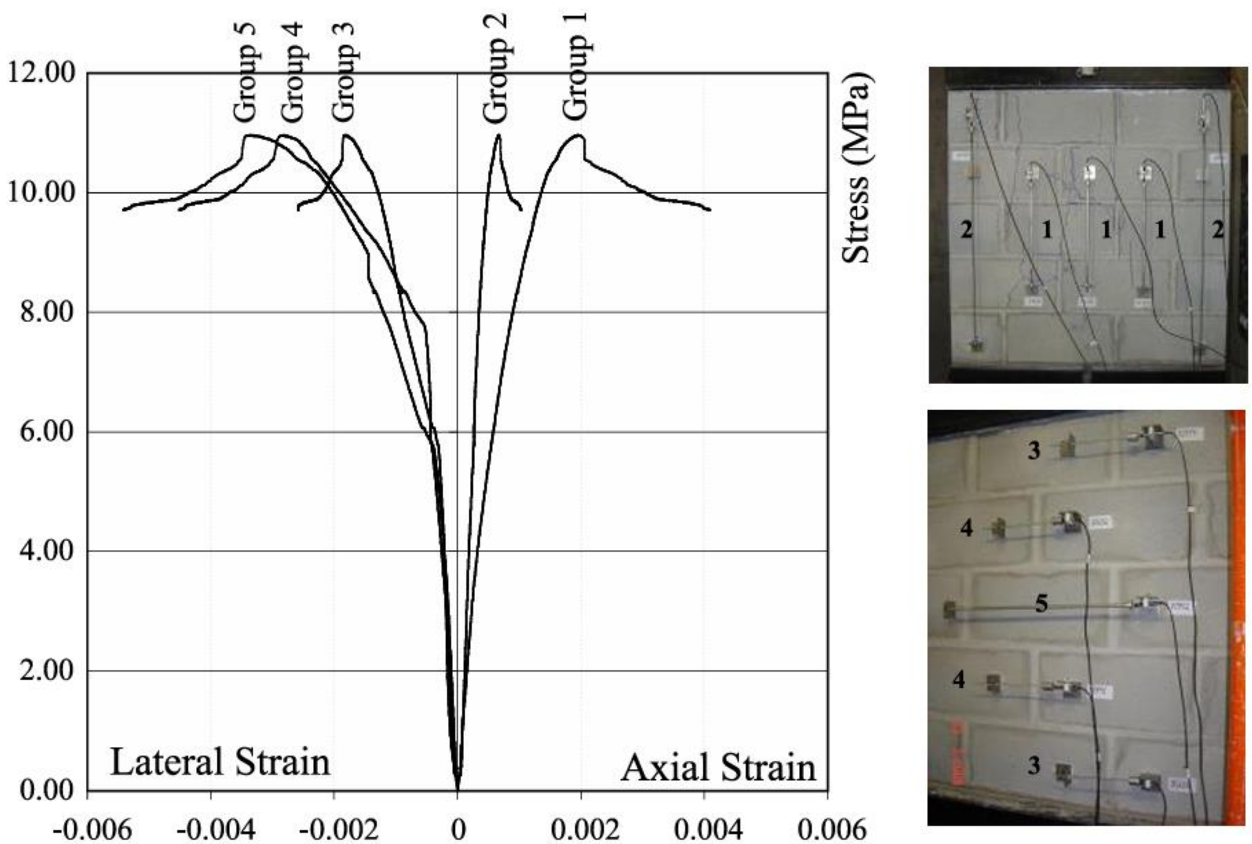

Figure 2.10: Axial and Lateral Stress-Strain Relationships of Type 2 Mortar Walls (Fonseca et al, 2015)

2.7 Effects of Capping on Compression Strength of Hollow Concrete Blocks

The capping of a brick is done to simulate the strength of the unit as if it were in a wall. This achieves a smooth perpendicular surface with no irregularities as this leads to local concentration of stress for compressive strength tests. A paper by Abaza et al. (2003) examined the effects of capping on the compressive strength of a Hollow Concrete Block in testing. This was achieved through cement-gypsum capping, as well as wood capping. Cement-gypsum was used over mortar cement capping because it creates a smoother and more consistent surface. One should note that the specimens tested had a thickness varying from 70 to 200 mm. However, the differences in size showed no significant effect on the compressive strength ratio; hence, a comparison can still be made. This is in contrast to the ones used in this dissertation which are 230mm thick.

The study concluded that no testing should occur without capping the brick due to the high variability in results caused by the uneven loading surfaces of the bricks, as this causes early cracking and local stresses. It also concluded that between cement-gypsum and plywood capping, both methods were valid and yielded consistent results; however, for stronger, thicker bricks, cement-gypsum is recommended, as it can withstand higher compressive loads. For further research it recommended that rubber be tried as potential capping. (Abaza et al, 2003)

2.8 Compressive Strength and Elasticity of Lime mortar and Clay bricks

Comparatively on an international scale more emphasis is put on the mortar joint with respect to clay brick masonry, as they are acting as a composite structure (Drougkas et al, 2015). There is a comparison to be made between the ratio of the elastic modulus and the compressive strength of the masonry. A considerable amount of research has been conducted on stack bond prisms and whole walls in terms of compression, as seen from the previous **Section 2.6** as well as most standards such as EN 1996-1-1:2005 only stating compression testing is needed for masonry units. However, there is significantly less literature on the composite action of brick and mortar, as well as their physical constituents, hence this presents a research gap, which this dissertation aims to investigate within the methodology of this research.

In this study, referenced by Drougkas et al. (2015), the primary aim of the research was to determine the compressive strength and Young's modulus of masonry made from medium-strength solid clay bricks and two types of low-strength lime-sand-based mortars, with no cement used. EN 1996-1-1:2005 estimates the masonry strength of a wall using the compressive strength of the masonry as the only parameter. This neglects other influences on the masonry, such as its constituent materials (i.e., the mortar, the unit itself, and its masonry composite properties). In terms of mortar samples, comparing free-standing samples and those in joint action reveals differences due to the deformation in the joints, which are relatively thin compared to a cube sample. The issue with the cube is the differing curing conditions, which do not match those of masonry. *(Drougkas et al, 2015)*

Hence in testing brick cores as seen in **Figures 2.11** and **2.12** were used to find the young's modulus and characteristic compressive strength as well as stack bond configuration for comparison. An advantage to coring was being more aware of the influence of local imperfections and for them to be measured or avoided. As for the tensile strength, 3-point bending was used. Two types of mortars were used that being ALM – Aerial Lime Mortar and HLM – Hydraulic Lime Mortar, both using a 1:3 lime to sand ratio, tested using EN 1015-11 with samples being cube prisms, tested both for flexure and compressive characteristics. (Drougkas et al, 2015)

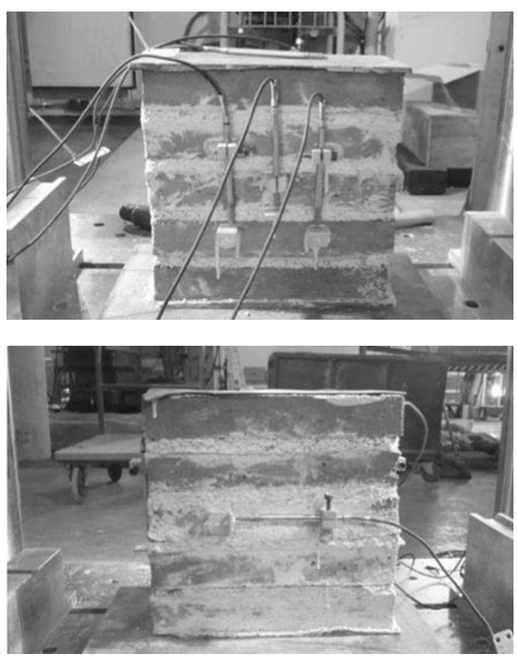

Figure 2.11: Vertical Cracks in Core sample (Drougkas et al, 2015)

Figure 2.12 : Testing Set up for stack bond configuration (Drougkas et al, 2015)

The main takeaways from the research being:

(1) Lime mortars can be used to achieve high masonry strength but were still slightly below the mortars covered in EN 1015-11 in terms of strength.
(2) The masonry strength was approximately ten times stronger in compression than the mortar.
(3) A lot of energy absorption in failure was possible especially in mortar crushing.
(4) The masonry composites had a higher compressive strength than that predicted in the EN standard. Whilst being consistent with the predicted increase in strength of masonry and mortar individually.
(5) The curing process is crucial for mortar in order for it to gain strength, as at 49 days the strength was much higher than those at 28 days.

Hence, the overarching takeaway from this study is that the brick is generally much stronger than the mortar, but the mortar itself still increases the strength of the brick. *(Drougkas et al, 2015)*

2.9 Conclusion

The design and testing of masonry walls are well standardised; however, there appears to be a gap with respect to the overarching effects of poor workmanship in laying mortar. Locally speaking, the effects of mortar tend to be overlooked. More studies have been conducted abroad on various materials but not on local materials and construction. Hence, researching the composite action of the mortar with the local block used could be beneficial for local construction.

It is important to note that design codes like EN 1996-1-1:2005 rely on simplified and linearised models of compressive behaviour, this may differ from real masonry which experiences more complex and variable situations with non-linear stress-strain response. The focus of this dissertation will be to find the relationship between the hollow concrete block work and the mortar present as well as the level of significance the strength of the mortar has upon the masonry unit. One should also note that there is limited literature available regarding the bending flexure of bricks, as well as research relating mortar placement to the failure modes of masonry. This is as most research carried out has focused on finding the flexure of bricks laterally due to wind, seismic loading, or when acting as a shear wall.

3. Methodology

3.1 Introduction

This chapter outlines the experimental procedure undertaken to investigate the mechanical properties of various wallettes. The objective of this research was to assess how varying joint strength, and placement can influence the compressive strength of masonry units.

Three different mortar mixes were initially tested; Mix A (M6, standard), Mix B (local “Xaħx") and Mix C (M2, standard). These were prepared using calibrated weighing of constituents and mixing. The water content was determined incrementally through trial and error until a workable consistency was achieved. This approach aligns with site practices, as no standards, such as BS EN 998-2:2016, recommend water content. Instead, the water content is left to the user's discretion. The aim was to produce a cohesive, plastic mortar suitable for masonry construction that exhibits minimal segregation and bleeding.

Mix A was chosen because it is the standard recommended mix in the local mason’s handbook (Camilleri 2023), Mix B was used as a comparison to standards such BS EN 998-2:2016 that specify an M2 and M6 mix, as contractors locally commonly use it. Mix C was used as a comparison to Mix A to determine how a reduced cement content affects the compressive and flexural strength of mortar. The testing regime for these samples consisted of 7- and 28-day compressive and flexural strength tests on mortar prisms, using six samples per mix.

The testing consisted of loading individual hollow concrete blocks (HCBs) and wallettes made from three HCBs with varying joint materials and joint configurations using neoprene, steel, and mortar. These variations were conducted to investigate the effects of joint strength, placement, and monolithic behaviour. Note monolithic behaviour is achieved from the bond of mortar on the block interface and its effects on the overall strength of the wallette

The intention behind this methodology was to create an exploratory comparative dataset across multiple variations. To find practical recommendations for masonry design and construction.

3.2 Mortar Mixes

Mix A

The Masons' Handbook (Camilleri 2023) and BS EN 998-2:2016 recommend that to achieve an M6 mortar class, one part cement and three parts sand are obtained by weight and mixed; however, the standards do not specify the water content. For mixing the samples, 1350 g of sand, 450 g of cement, and 500 ml of water were used based on trial and error.

Mix B

Camilleri (2023) states that a mortar mix, locally known as "Tajn Mielaħ", is commonly used by local contractors. This mortar consisted of a mixture of one part cement, two parts sand, and six parts Limestone dust (Xaħx), obtained by weight and mixed; standards do not specify the water content. For mixing the samples, 1350 g of Xaħx, 450 g of sand, 225g of cement, and 600 ml of water were mixed based on trial and error.

Mix C

BS EN 998-2:2016 which recommends for an M2 mix, one part cement and four and a half parts sand are obtained by weight and mixed together, standards do not specify water content. For mixing of samples 1350 g of sand, 300 g of cement and 500 ml of water were mixed based on trial and error.

3.3 Mortar Testing

EN 1052-1:1999 describes the mixing procedure for mortars and provides flow values in accordance with EN 998-2:2016 and EN 1015-3:1999, along with guidance on fresh properties according to EN 1015-7:1999. EN 1051-11:1999 is critical as it defines the standardised test method for determining the flexural and compressive strength of hardened mortar specimens, that EN 1052-1:1999 directly adopts. The fresh mortar sampled will have a minimum volume of 1.5 times the volume needed for testing; this is done to account for any losses during the casting of moulds and jolting. Such samples will be obtained by reducing the bulk test sample as per EN 1015-2:1999, which outlines the bulk sampling of mortars and the preparation of test mortars.

3.3.1 Mortar Sample Preparation

As a general guideline, BS EN 1015:1999 Methods of testing for mortar for masonry and all its parts were used for the testing procedure of mortar samples. In total, eighteen prisms were prepared, six per mix, three tested for the 7-day tests and three for the 28-day tests. The test samples, 160 x 40 x 40 mm (± 1 mm), were prepared. Each constituent of the mix was weighed in a container of known mass, and the weights were recorded. The mortar mix constituents were placed in a mixer, and water was added till a visually usable mix consistency was obtained. The mix was then placed in steel moulds, and the moulds were lubricated with oil to prevent adhesion of the mortar. Each sample of mortar was properly compacted by hand at least ten times into the moulds, which were then vibrated via a jolting table. This procedure was adopted to create a uniform, consistent mortar test sample with no air entrapment and segregation of the mix. The samples were then sealed in transparent polyethylene laboratory film and left to cure, as seen in **Figure 3.1.**

Figure 3.1 Mortar Moulds

3.3.2 Flexural Strength Tests of Mortar Mixes

The prism samples were demoulded after one day, as shown in **Figure 3.2**, and then marked and stored in a water storage chamber. This decision was taken as an interpretation of the standard via Table 1 of BS EN 1015-11:1999, which it states :

"Storage chambers, capable of maintaining a temperature of 20 °C ± 2 °C and a relative humidity of 95 % ±5% or 65% +/- 5%".

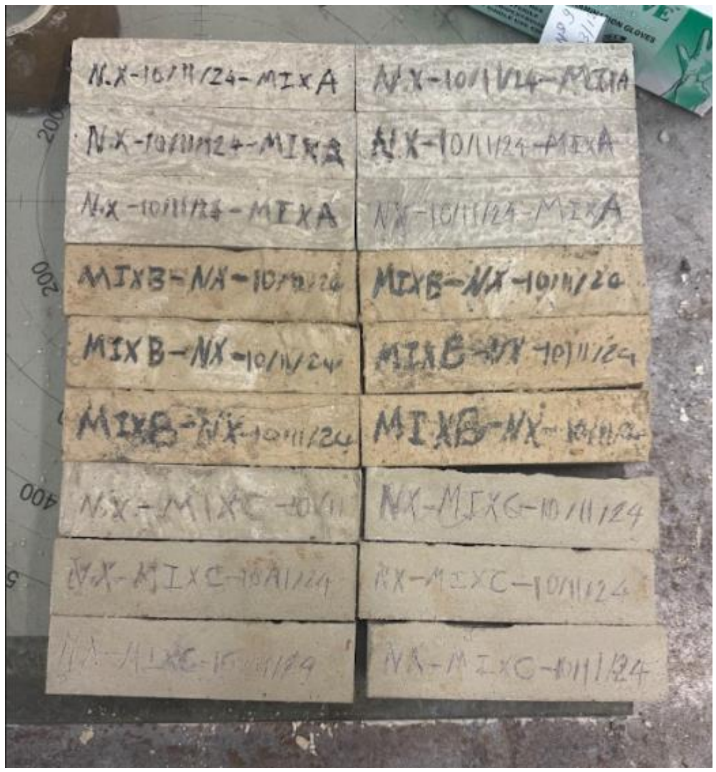

Figure 3.2: Mortar Prisms Tested

Hence, the samples were kept in a water chamber as it can be taken as 100% humidity up till the 7-day tests. After which, for the remaining time the samples were kept in the lab in air at a 65% +/-5% humidity until being tested at 28 days. The 7 and the 28-day tests were carried out using the following testing procedure. The prisms to be tested, were marked at the centre of the sample, another two lines were made at 50mm on each side of the centre. These lines were used to position the sample in the 3-point bending test. A total number of 18 specimens were tested in flexure, for both the 7 and the 28-day tests. The loading rate applied for the flexural test was 50 N/s, conforming to EN 1015-11:1999.

The load is applied uniformly over the width of the prism, such that through its length it is acting as a point load at the centre point of the specimen. The maximum load to cause flexural failure was recorded and the broken specimen kept for the compressive strength test. The test apparatus seen in **Figure 3.3** consisted of steel supporting rollers and the test specimen prism, with the third roller on top apply the flexural load. The rollers remained equidistant and can tilt slightly to avoid torsion and uneven stress distribution. The tilt accommodates for any minor misalignments or unevenness in the samples.

Figure 3.3: Three Point Flexure Test

The flexural strength was then calculated using equation 3a:

$$f = 1.5 \cdot \frac{F \cdot l}{b \cdot d^2}$$ **Eqn 3a**

where: *F* *force applied*

b *breadth of the mould*

d *depth of the mould*

l *the length between rollers.*

3.3.3 Compressive Strength Tests of Mortar Mixes

From the 18 flexural test specimens, 36 compression test samples were obtained, as seen in **Figure 3.4.** These halved samples were then tested in the compressive test machine shown in **Figure 3.5**. The compression contact area was 40 x 40 mm, for both the 7- and 28-day tests. A loading rate of 2400 N/s was applied to the specimens up to failure. The maximum load obtained was recorded.

Figure 3.4 : Mortar compressive test samples obtained after flexural tests

Figure 3.5: Mortar Compressive Test Set Up.

The compressive strength was then calculated using the following equation 3b:

$$R_c = \frac{F_c}{1600} \qquad \textbf{Eqn 3b}$$

where   *Fc*   *compressive force*

3.4 Compressive Strength of HCB Unit

This section outlines the procedure followed to determine the compressive strength of individual hollow concrete block (HCB) units. Detailing the preparation of the blocks by capping of the top and bottom faces, ensuring uniform load distribution, and how to find the respective peak compressive stress for the unit. These tests provide a baseline strength value for the blocks which is essential for the comparative analysis of the wallettes, as it acts as a control.

3.4.1 Capping Procedure

One hundred and twenty HCB units were obtained from a local manufacturer; the dimensions and configuration of the HCB units can be seen in **Figure 3.6**. In order to have a uniform bearing surface the blocks were capped to provide a uniform smooth level surface. The capping has a thickness between 3 and 5mm. The blocks were measured, and formwork as seen in **Figure 3.7** was made for capping purposes. The internal 5mm taper from top to bottom was accounted for hence two plug templates were made. The plugs being made out of PETG to withstand the heat of hydration of the capping process, whilst the lengths were made from aluminium. To prevent adhesion of the grout onto the form work prior to casting they were lubricated via oil.

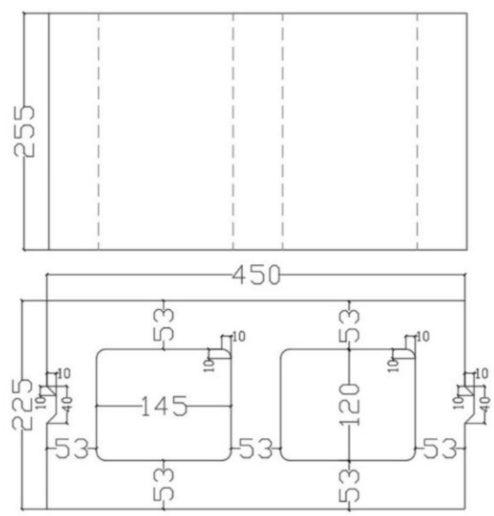

Figure 3.6: Blocks Used for Testing

One should note that fibreboard is no longer accepted as a capping medium for block testing for standard compressive tests as it alters the measurements for displacement due to not having a high enough stiffness in comparison to the brick. Whilst when capping with a non-shrink grout it does not affect the measurements of displacement.

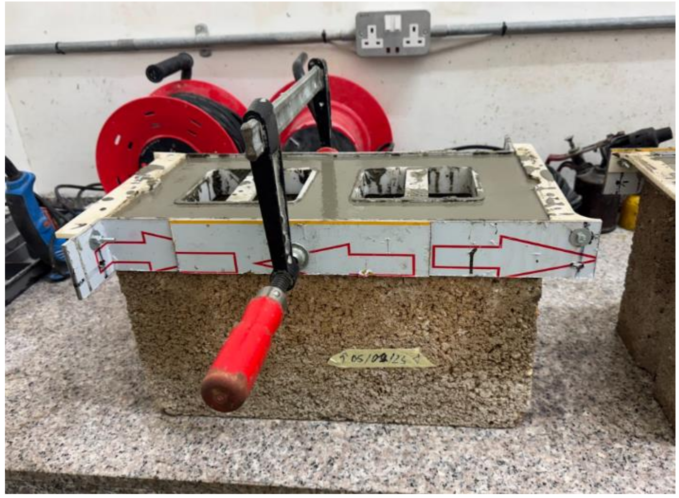

Figure 3.7: Capping Moulds and Set-Up

As a guideline the capping procedure BS EN 772–1:2011; Section7.2.5 was used, changes being made to account for tolerances. For example, using g-camps as well as putty to prevent leaking during the casting. In accordance with EN 1015-11:1999, the capping mortar had to have a minimum compressive strength of 30 N/mm^2, a non-shrink grout SIKA 312 was used as it has a compressive strength of 40 N/mm^2 after 1 day of curing. The spec sheet recommends using 3.3 - 3.4l of water per 25kg, one cap is approximately 1 kg of sika hence the water ratio proportionally changed for scale. Through trial and error, it was found that the ideal water content was 175~185ml, for workability, flow and self-levelling. The grout needed to be self-levelling so that a near perfectly flat finish could be obtained, as seen in **Figure 3.8**. The blocks were placed on a smooth level surface, prior to pouring the grout, the faces were pre moistened to as to ensure proper adhesion between the surface and the capping grout.

Figure 3.8 : Capped Hollow Concrete Block

3.4.2 Compressive Testing of Single Brick Unit

Once the blocks were capped, they were left to cure in air and then stored for testing. For the block compressive tests both the top and bottom surfaces of the block were capped. The blocks were weighed and dimensions measured. Six blocks were initially tested to failure, after which four blocks were white-washed and tested, the white-wash in this case was applied so that initial cracks could be observed. The blocks were tested in accordance with Table 2 of BS EN 772-1:2011 the loading rate used was 0.05 $N/mm^2/s$ as the expected strength was less than 7 N/mm^2. As the capped faces were plane and parallel this allowed for the load to be applied across the full contact area using steel platens on the compression rig, as seen in **Figure 3.9**. The maximum compressive stress obtained was then found by applying the maximum compressive force over the gross area, taken as 225 x 450 mm. The gross area of 101,250 mm^2 was kept the same throughout all the testing, even for the wallettes as a 1:1 comparison with respect to stress as opposed to the net area, due to changing contact areas.

Figure 3.9 : Compressive Test Set Up of Hollow Concrete Blockwork.

3.5 Wallette Testing

The aim of these tests was to obtain values for compressive load and relative end displacement such that graphs can be plotted for stress and strain. In this manner one can analyse the effects of joint strength and placement on the compressive resistance of HCB wall construction.

Ideally three tests at minimum would be carried out per case, in doing so the coefficient of variation, standard deviation and mean of the test results could be observed. However, it was decided that the research present would be of a more explorative nature hence a number of joint variations and strength were investigated.

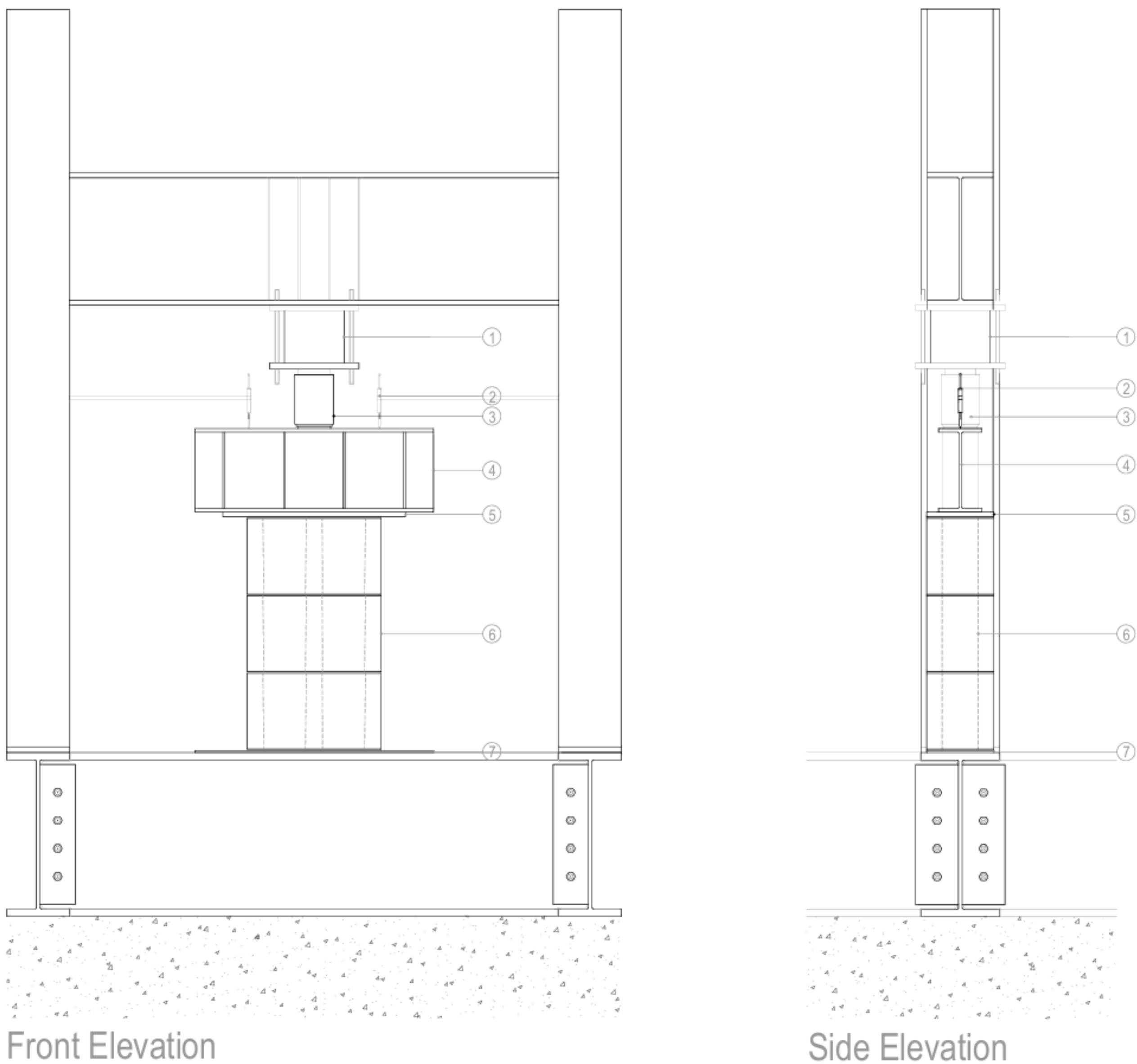

Figure 3.10: Compression Rig Set-Up at UOM Laboratory

1. **Hydraulic Jack:** This was used to simulate the vertical loads experienced in local construction.

2. **50 mm – Linear Variable Differential Transformer - LVDT:** These were used to measure the relative displacement of the joints taken as an average between the LVDT's. As they were placed on top of the spreader beam to avoid damaging the equipment, the displacement was divided equally between two joints.

3. **1000 kN Load Cell:** This records the load upon the wallette. It was calibrated up to a maximum load of 1000 kN prior to testing. In testing it was connected to a data logger which recorded the loads at intervals in Kilo Newtons.

4. **Spreader Beam:** This spreader beam ensured that the load would be uniformly distributed along the area of the wallette.

5. **Top plate:** This 10 mm plate was used to further dissipate the load coming from the steel spreader beam, as the spreader beam is not perfectly as wide as the wallette. It also allowed for ease of placement of the spreader beam.

6. **Wallette:** The wallette was varied in terms of joint properties and capping but all wallettes were made from three 230mm double type Hollow Concrete Blocks.

7. **Bottom plate:** This 6mm plate was used to allow for hollow concrete block placement at the bottom, in order to adjust and make sure that the wallette is placed centrally. It makes part of the steel casing in case lifting of the wallettes is required. In terms of dimensions, they are 200 x 800 x 6 mm steel plates with 12 mm holes at the corners.

3.5.1 Calibration of Equipment

The LVDT – Linear Variable Differential Transformer used for the test set up has a resolution of 0.01 mm as seen in **Table 3.1**. The LVDT was calibrated for 50 mm range of travel. This was done using micrometre and a pulley with known weights. This correlates the displacement measurements incrementally from the LVDT with the data from the strain gauge under known loads, as seen in **Figure 3.11**. This method ensures accurate alignment between displacement and electrical output.

Specification	Parameters
a) Respective Measurement Range	10 mm, 25 mm, and 50 mm
b) Resolution	<= 0.01mm or better
c) Non-linearity	≤ ±0.25% of rated output
d) Output Voltage	0 to 5 V
e) Frequency	≥ 10 kHz
f) Operating temperature	=-20C to 70C

Table 3.1 LVDT Specification

Figure 3.11 : LVDT Calibration

The 1000 KN load cell was calibrated up to 950 KN, at a sensitivity allowing for intervals of 50 KN. This was done by placing the load cell in a compression machine, as seen in **Figure 3.12.** The load cell was positioned centrally on the loading platens to ensure axial alignment. A load was applied at intervals and compared to the values obtained from the load cell when the values match it is well calibrated.

Figure 3.12 : Load Cell Calibration

3.5.2 Wallette Construction – Neoprene and Steel

In all materials, the placement scenarios were:

(a) Transverse Full (b) Shell Bedding (c) Ends Only (d) Fully Embedded

There were four different placement typologies for both materials as observed in **Figures 3.13** and **3.14.** Each material having a thickness of 5 mm to mimic the 5 mm mortar joint. The steel joint representing an overly stiff mortar whilst the neoprene representing an overly soft mortar. Every wallette being made of three double capped bricks on top of each other aligned to the load cell above it. Said wallettes being constructed manually in the pit. Note that due to the soft nature of the Neoprene its pre-compression upon its own self weight in terms of displacement was noted and accounted for in strain calculations.

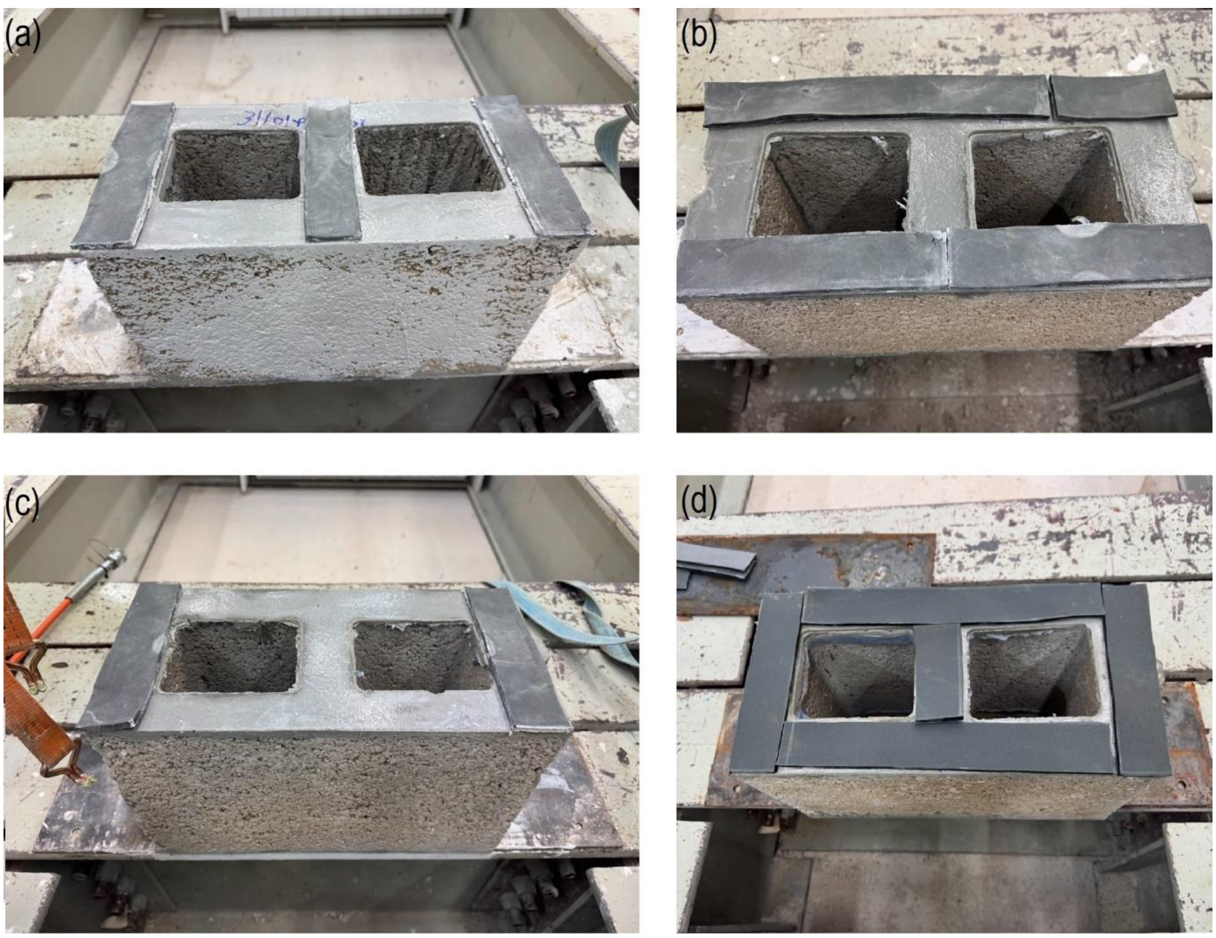

Figure 3.13: Different Neoprene Placements

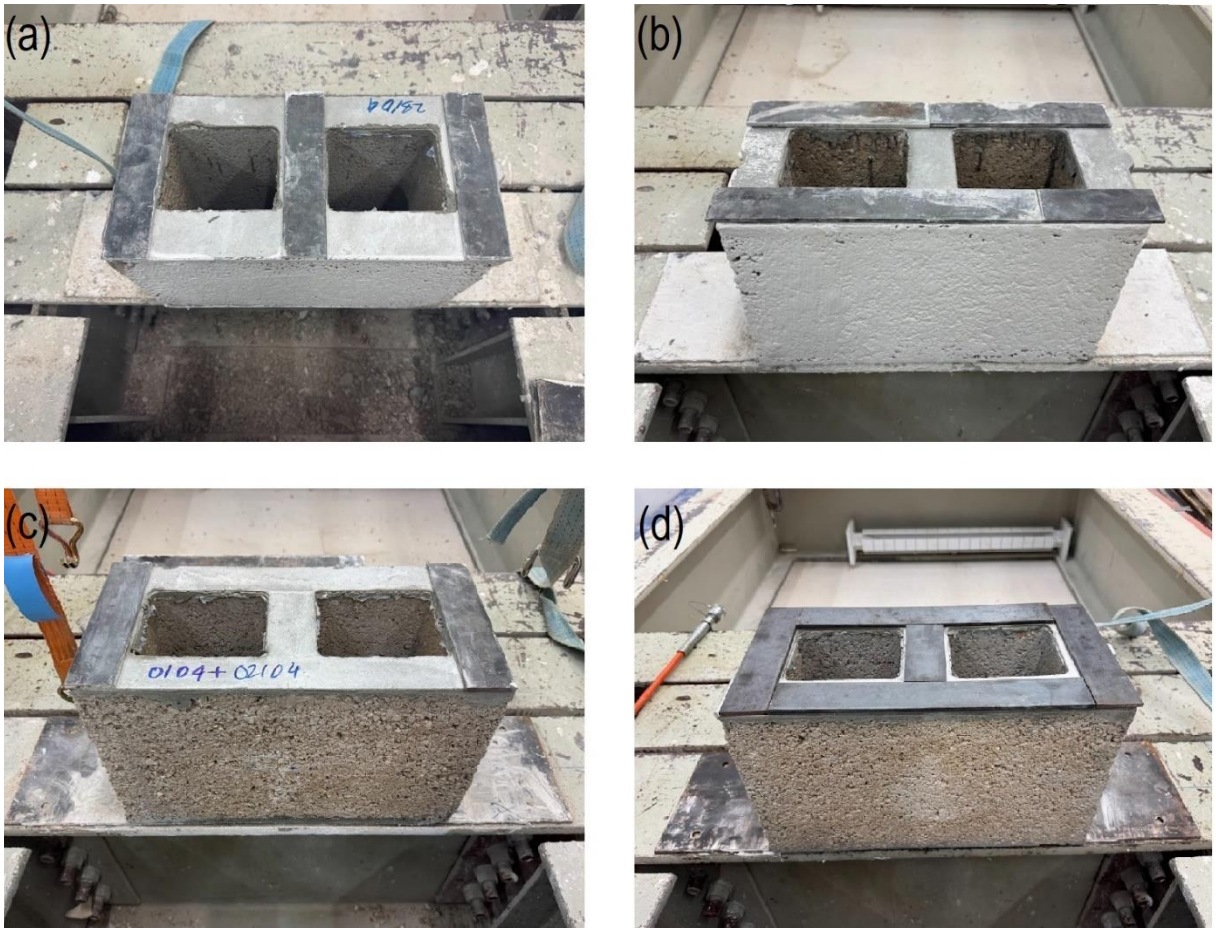

Figure 3.14: Different Steel Placements

3.5.3 Wallette Construction – Mortar

The tests focused on the M6 mortar case as this is the mix specified by the local standard as well as that of a building with a seismic mortar, has to be at minimum M5. There were four different placement typologies for mortar as observed in **Figure 3.15.** In this case the top and bottom bricks are capped on one side at the interface, as to compress against the steel spreader beams whilst the middle brick has no capping to allow for adhesion with the mortar. An extra set of tests were further conducted with the mortar placements to check the effects of adhesion and bond at the interface via use of double capped bricks, to mimic reduced adhesion. In this case adhesion refers to the bond strength developed between the mortar and the surface of the block. By filling the interface voids with a SIKA 312 capping taking the mortar's place, this adhesion is reduced considerably.

Each brick being placed carefully and wet prior to application of the mortar. The bricks were checked to be level after the placement of each brick, using a level ruler ("invell"). In order to ensure a 5mm joint, steel spacers were used. In all cases, once the steel spacers were removed mortar was packed into the voids post placement of the brick. The mortar being placed via trowel and the brick being compressed onto the mortar via the traditional "pal" for compaction and levelling.

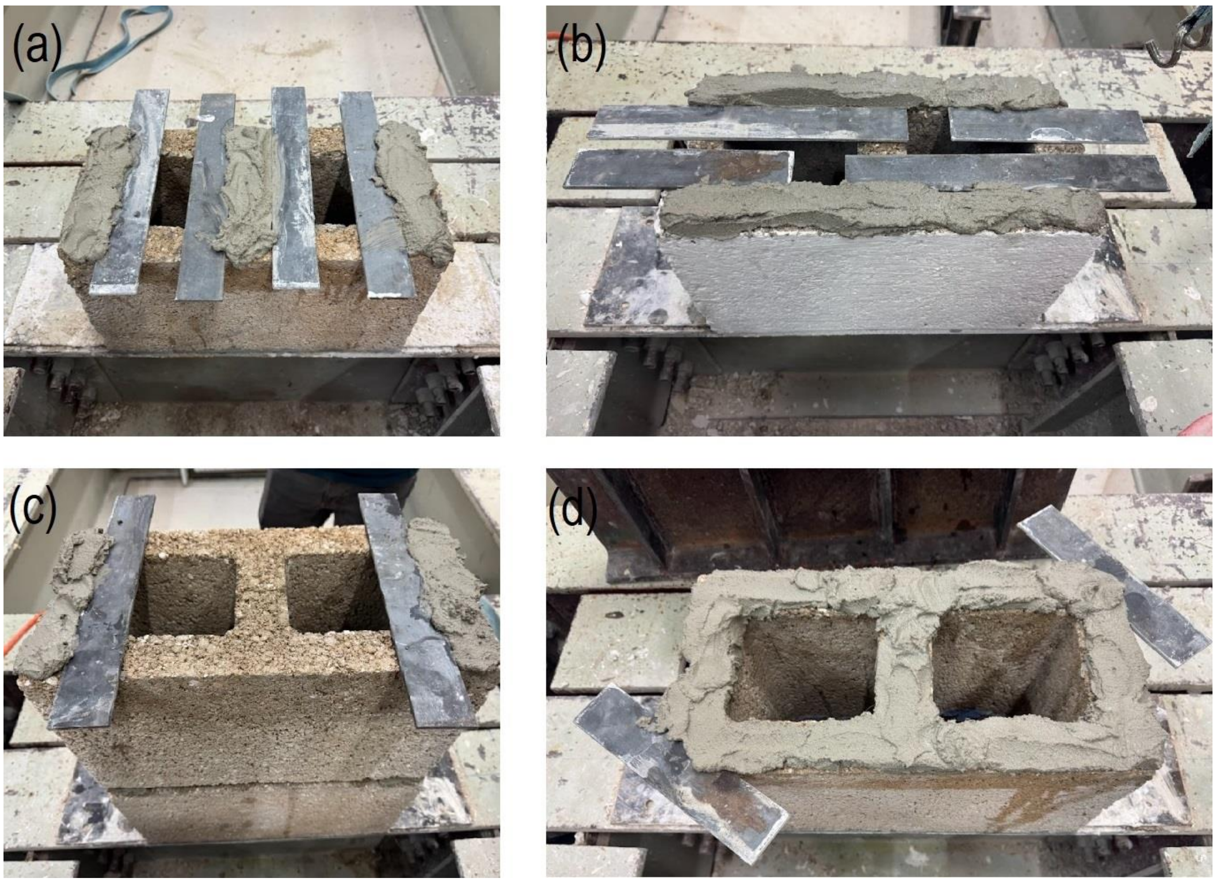

Figure 3.15: Different Mortar Placements

3.5.4 Testing Procedure

For the testing procedure of the wallette samples it was decided that a loading rate of 50 KN/minute would be used in order to see crack propagation as it occurred over time, as opposed to crushing it to failure load immediately. This decision was done following BS EN 1052-1:1999 which states that if the block tested is likely to fail prematurely if loaded too quickly it is ideal to apply the load slowly. This was done to not only understand the wallettes' ultimate load but also its serviceability limits. Note that the mortar wallettes were also given a curing time of three days to reach the specified strength (M6), as extrapolated from the results of the initial mortar tests. When possible, mortar cubes were done using excess mortar from construction of the wallettes to see what the actual strength of the mortar was on the day of testing

The slow loading rate also gave time for the LVDTs to note the displacement and load cell to note load, both being connected to a data logger to record each test. The LVDTs output displacement readings are based on the movement of its core, hence the starting value varied based on its compression. Hence the cumulative relative values of the data set gave the displacement of the wallette, whilst the load cell was set to read the load in kilonewtons.

The specimens were built in the pit itself and placed centrally in the compression rig and were white-washed with plaster to note when initial cracks occurred. The plaster was generally given a day to cure. As the wallettes were being loaded at intervals any cracks were marked at the load via pencil, at higher loads this was not possible due to safety concerns of sudden failure. The compressive force being applied at intervals was kept constant for 1 minute and raised 50KN until the failure of the wallette occurred, after which the rig is released so the debris can be cleaned and carted away. Failure was considered to be the point at which the wallette could no longer sustain higher stresses, as opposed to full crushing. As a safety precaution straps were tied around the spreader beam in case of sudden failure of the wallette.

3.6 Set-Up Limitations

A testing limitation was attributed to the displacement logging of the testing via the LVDTs, their placement on top of the LVDT is not ideal, as it is not directly measuring the displacement of the joint. Ideally four LVDTs were set up two per joint on the face of the wallette to directly measure displacement of each joint. One should also note that in failure the spreader beam would tend to rotate due to the wallette failure or partial collapse of one side. Hence lifting one LVDT up and pushing the other LVDT down which would not be an accurate representation of the displacement actually occurring at the joint.

Another limitation being the hydraulic jack used, as this jack is worked manually when pressure is added it was hard to have exact intervals of 50 kN precisely. A primary limitation throughout the entire process was limited time and resources, as ideally more tests were conducted with more samples to have a mean average for comparison of data. This is as a large amount of the data collected per wallette variation was only done once.

An inevitable limitation being human error throughout the entire process. The capping of the bricks were not perfect as approximately 120 brick faces were capped, hence with that large amount of casts there was bound to be some error. As well as the placement of the bricks, they were measured, placed and levelled out as accurately as possible but some inherent eccentricities were present. One should also note the quality of the bricks was quite poor, which inherently affected the set up and testing of the wallettes.

Finally, a limitation was that for compression of the mortar samples and the single hollow concrete blocks, the compression rig in question had no method of measuring displacement and solely measured stress. It was also not possible to add LVDTs to the set up in question.

4. Results

4.1 Introduction

This chapter presents and analyses the experimental results obtained from the exploratory research into the compressive behaviour of hollow concrete blocks, mortar prisms, cubes and wallettes. The aim is to understand how joint strength and placement affect the overall performance of masonry under axial loading. The chapter is structured to initially examine the individual components of the wallette as a base line, starting with the block unit and followed by mortar testing. These initial results are then compared against the performance of the wallettes. A total of 18 wallettes were tested, with results being tabulated and plotted as stress-strain curves for comparison. The findings were also compared to design principles defined by EN1996-1-1:2005 such as equation 3.1 and material partial safety factors to evaluate how well the code aligns with actual raw experimental data, that would lead to practical insights into workmanship.

4.2 Hollow Concrete Block Single Compressive Testing

The loading rate used was 0.05 N/mm^2/s, to calculate the stress an area of 101,250 mm^2 was taken being the gross area. The gross area was chosen as a base line to be applied on the wallettes for comparison of data. The results from the compressive strength testing of ten individual hollow concrete blocks are presented in **Table 4.1.** The compressive strength values ranged from 5.33 MPa to 6.32 MPa, with a mean value of 5.828MPa. The coefficient of variance in this case was 12% this indicates a moderate level of variance, with the mean strength still being lower than the expected 7MPa which is the industry standard, being 16.74% lower. This overall indicated the blocks were not of the highest standard and quality. One should note that the initial cracks varied too much with a high coefficient of variance of 58.70% hence these values were dismissed.

Often the HCB units failed in a similar mode showing internal degradation and vertical splitting cracks along the internal “web” regions of the block, as seen in **Figure 4.1.** One should also note there were cracks along the length of the blocks which were difficult to capture due to the rig set up. The cracks initiated at the surfaces interacting with the steel platens of the rig and slowly propagated, meeting in the middle leading to failure. Any sudden failures were due to stress concentrations caused by unseen internal voids. Hence it can be said that the main failure mode was brittle axial splitting along the HCB web, with local crushing due to stress concentrations.

Brick Sample	Height	Length	Width	Weight
	mm	*mm*	*mm*	*kg*
A	265	450	226	34.385
B	265	450	226	35.18
C	265	450	225	35.375
D	265	450	226	35.725
E	265	450	225	34.87
F	265	450	225	34.925
G	265	450	225	36.19
H	265	450	225	36.17
I	265	450	225	35.055
J	265	450	225	35.01
Average	265	450	225.3	35.2885
Brick Sample	**Date tested**	**Max Load**	**Max Stress**	**Initial Crack**
		kN	*Mpa*	*Mpa*
A	02/04/2025	483.8	4.78	/
B	02/04/2025	617.5	6.1	/
C	02/04/2025	626	6.18	/
D	02/04/2025	588.6	5.91	/
E	02/04/2025	548.5	5.42	/
F	02/04/2025	666.2	6.58	/
G	29/04/2025	540.3	5.34	2.5
H	29/04/2025	666.2	6.22	1.65
I	29/04/2025	451.4	4.46	1.65
J	29/04/2025	548.1	5.41	5
Average		573.66	5.828	2.7
Standard Deviation		/	0.67	1.58
Coeffecient of Variance		/	11.79%	58.70%

Table 4.1: All 10 Hollow Concrete Block Test Values

Figure 4.1: Specimen G Crushed Block in Compressive Rig, Failure @5.34 MPa

4.3 Mortar Test Results

The 7- and 28-day prism test results indicated that standard mix recommendations achieve higher strength than specified, as seen with Mix A (M6) and Mix C (M2). After 7 days, the M6 and M2 mixes already had a minimum strength of 12 MPa and 3.8 MPa, respectively, as observed in **Figure 4.2.** This indicates that the standards conservatively recommend a mix that, at minimum, gives the specified strength. The 28-day test results further strengthened this viewpoint, with the M6 and M2 mixes having a mean compressive strength of 24.8 MPa and 7.895 MPa, respectively.

Mix B, being the "Xaħx" mix, had the lowest compressive strength of 2.52 MPa. The Xaħx mix being the weakest is concerning, as established in the literature review by Bartolo et al, (1991) it is the typical local practice to use Xaħx in mortar mixes due to its workability, as well as it's being cheap and broadly available.

Notably, both M6 and M2 mixes achieved four times the specified strength, suggesting that the standard could be over-specifying the mix strength, whether this is intentional or not, is not clear. This could be done to account for variations in water content and working conditions. According to EN 1996-1-1:2005, the minimum mortar strength for masonry under seismic loading is M5; therefore, an M6 mix was used for the main testing of the wallettes to ensure the results of the mortar wallettes have more practical application.

From the initial mortar prism compressive test results of Mix A (M6) , via extrapolation as seen in **Figures 4.2 and 4.3** , it was decided that an M6 mortar would be achieved at around 2.5-3 days; hence, it was tested within that range. To check that the mix was actually M6 within this curing range, a total of 17 cubes were tested during the production of nine HCB wallettes. These tests had a high coefficient of variance 29.46% in comparison to the 7- and 28-day tests, which had coefficients of variance of 10.90% and 1.94%, respectively, both based on 6 samples each, as seen in **Figure 4.4 and 4.5.**

The variation in compressive strength of the mortar is due to multiple factors. The prism samples were all from the same batch and were cured in water for a week, then allowed to air dry in a controlled environment i.e. a sealed room. However, the cubes were cured in a more variable environment i.e. the lab pit next to the wallettes and made over multiple weeks using different batches. The prism mix was made with a ratio of 1350 g sand, 450 g cement, and 500 ml water; however, for each wallette, these quantities were scaled proportionally based on the required mortar volume whilst maintaining the same mix ratio.

This change in batch size led to variation in water content, which changed the mix properties. The prisms were jolted and compacted, in contrast to the cubes, which were hand-packed via trowel. The cube tests showed that, on average, the mortar gained strength rapidly after 3 days, being stronger than the anticipated 6 MPa. It could be the case that the M6 mix specification is a conservative minimum however there is no official statement declaring this within the code. However, it still remains the case that when a 1:3 mix was used in testing it was much stronger than 6 MPa. Hence, the HCB wallettes were made with a mortar material that is stronger than the brick itself.

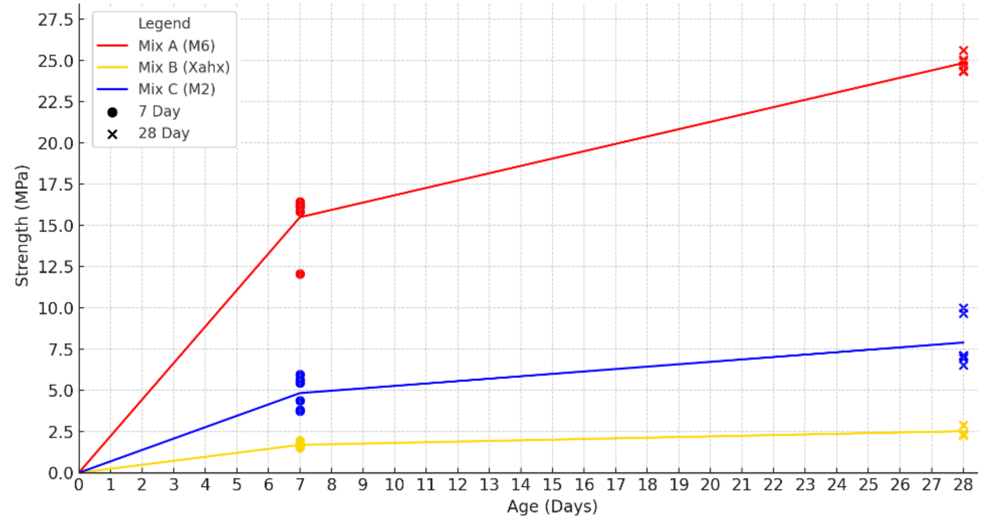

Figure 4.2: Compressive Half Prism Tests Values of Mixes A,B and C

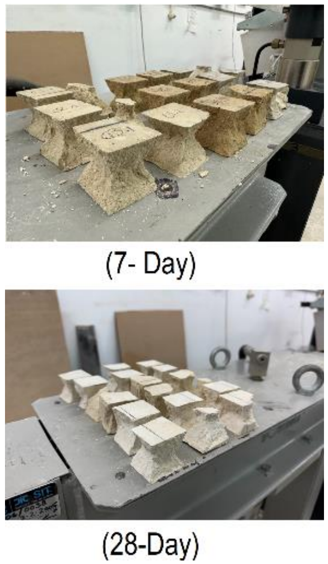

Figure 4.3: Crushed Samples

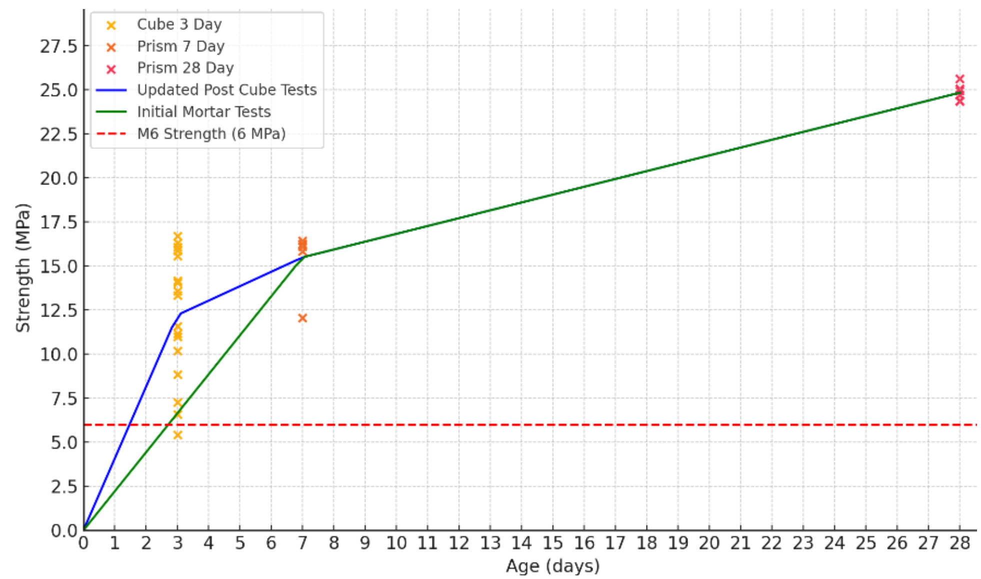

Figure 4.4: Updated M6 Compressive Values with Cube Tests

Figure 4.5: Cube Test Results

4.4 Sensitivity of Equation 3.1

This section investigates the influence of the main variables on the output of Equation 3.1 that being the characteristic compressive strength of a masonry unit f_k. This is done by first varying the compressive mortar strength f_m and keeping the compressive block strength f_b constant and inversely with varying the f_b and keeping f_m constant. This provides insights into the respective contribution of each component as well as the implications of Eurocode design.

4.4.1 Variation of Mortar Strength

To understand how varying mortar strength affects the design characteristic compressive of masonry f_k, equation 3.1 from EN 1996-1-1:2005 was used: $\mathbf{f_k = K \cdot f_b^{\alpha} \cdot f_m^{\beta}}$

Where f_b is the mean compressive strength of the block unit,

f_m is the mean compressive strength of the mortar,

K, α, and β are constants depending on the unit and mortar type.

In this case the constants were $\alpha = 0.3$, $\beta = 0.7$, and $K = 0.45$ via EN 1996-1-1:2005, Table 3.3 as it is a group 2 aggregate concrete block using a general-purpose mortar via EN 1996-1-1:2005.

A parametric analysis was done by plotting three lines using different values of f_b to observe the effect of varying f_m on f_k, as seen in **Figure 4.6;**

(i) Using f_b = 7 MPa, the industry standard

(ii) Using f_b = 5.828 MPa, the tested mean compressive strength of the hollow concrete blocks from **Section 4.2.**

(iii) Using f_b = 3.5 MPa, the standard strength taken for light partitions.

This allowed for the analysis of how sensitive f_k is to changes in f_m and confirmed that whilst mortar does influence f_k, f_b remains the dominant factor due to it having a higher exponent of 0.7. The purpose of said analysis was done to see how realistic the Eurocode's design recommendations are when compared to actual test data, from **Section 4.3.**

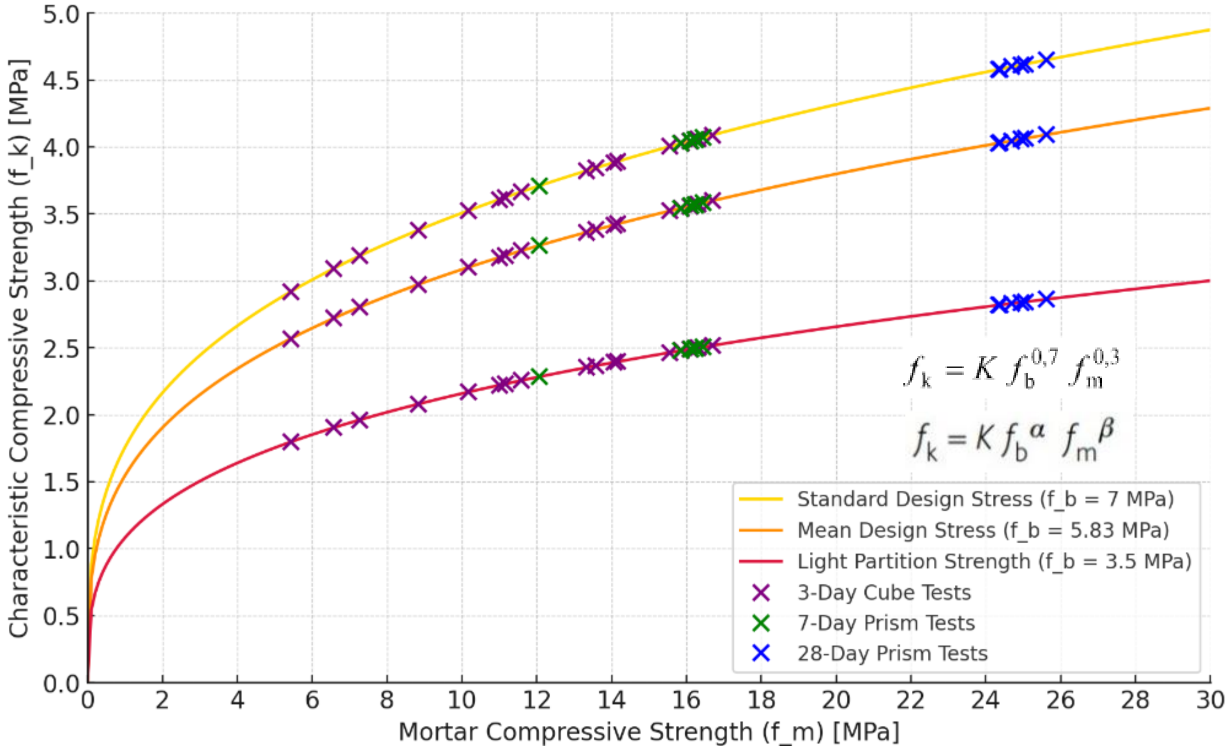

Figure 4.6: Characteristic Compressive Strength f_k against Mortar Strength f_m with f_b Constant

The graph shown in **Figure 4.6** indicates the output of the equation f_k is more sensitive to block strength f_b than that of the mortar strength f_m. Through the application of Equation 3.1 from EN 1996-1-1:2005 , it is observed that as f_m increases, so does f_k at a rapid rate; as it is reduced, it becomes more linear. For example, when f_b = 5.828 MPa, increasing the mortar strength from 6 to 12 MPa results in an increase of approximately 0.54 MPa. However, increase f_m further from 12 to 25 MPa yields a similar increase of 0.54MPa, despite doubling the mortar strength. This demonstrates diminishing returns in f_k at higher mortar strengths due to lower influence on f_k. This trend was consistent for the 3, 7, and 28-day mortar results. This indicates that Equation 3.1 EN 1996-1-1:2005 can be used at different curing ages, provided that the corresponding compressive strength of the mortar at each age is known. This would align with the realities of construction, in which on-site workers do not wait for mortar to cure to its full strength before loading it with the spanning beams, slabs or more masonry. At higher mortar strengths, when f_m exceeds f_b, the gains in f_k diminish. This diminishment is a result of the exponents in Equation 3.1 of EN 1996-1-1:2005, where the block strength f_b has a greater influence than the mortar strength f_m . This influence highlights that the unit strength is the dominant factor in EN 1996-1-1:2005.

4.4.2 Variation of Block Strength

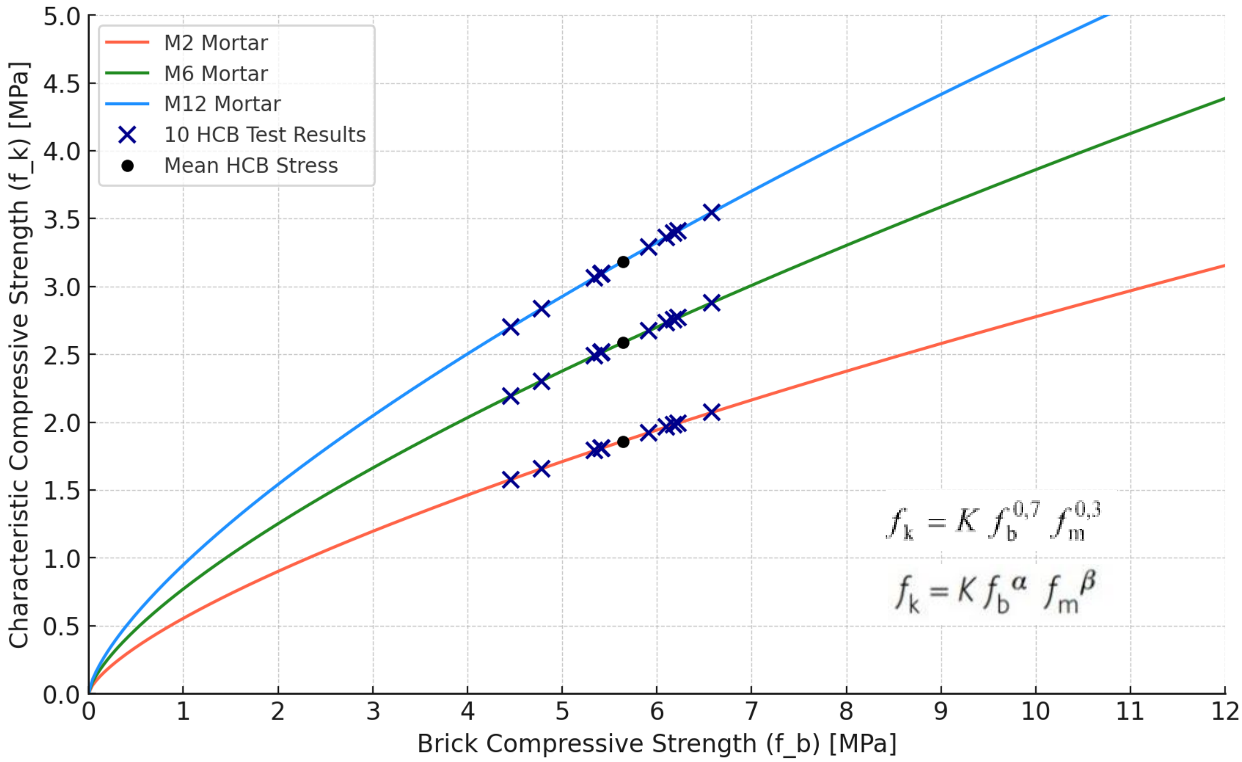

Figure 4.7: Characteristic Compressive Strength f_k against Block Strength f_b with f_m Constant

As a control for the initial plot, a second graph was plotted using equation 3.1 of EN 1996-1-1:2005 as seen in **Figure 4.7**, varying brick strength while keeping mortar constant, producing three curves for M2, M6, and M12 Mortars with the same constants as prior in terms of α, β and K. This comparison demonstrates that Equation 3.1 EN 1996-1-1:2005 gives greater influence to block strength than mortar strength, as seen from the steeper and more linear response in f_k when varying f_b in **Figure 4.7** when compared to the response when varying f_m in **Figure 4.6.** Hence f_k is more sensitive to f_b. The tested single HCB values were also noted on the lines for comparison.

From a EN 1996-1-1:2005, design perspective, this highlights the practical importance of block quality control in masonry construction. This is in contrast to mortar, which indicates that for higher strengths, the gains are smaller, while increasing f_b directly leads to increased gains in f_k. The block dominance is computationally due to the exponents applied to the brick strength being 0.7, while for the mortar strength, it is 0.3. Hence, from first principles, it will always be the case that the block strength has a more significant and direct influence.

For example, increasing f_b from 5 to 7 MPa at a constant M6 mortar leads to a 0.7 MPa increase in fk, whereas doubling the mortar strength from 6 to 12 MPa at a constant brick strength of 5.828 MPa results in a smaller 0.4 MPa gain. Overall, this reinforces the notion that block strength is the primary factor influencing f_k in Equation 3.1 (EN1996-1-1:2005), and that increasing unit strength is more effective for improving masonry performance than using excessively strong mortars.

As discussed in Chapter 2, this conclusion is further supported by Fonseca et al. (2017), whose research exemplified that while mortar strength influences failure mode and stress distribution, the compressive capacity of masonry is still largely governed by unit strength which is reflected in equation 3.1 (EN1996-1-1:2005).

4.5 Wallette Test Results

A total of 18 tests were carried out within the research; however, each case was carried out at minimum once, which is insufficient to establish variations that may occur. The research conducted is exploratory and aimed at understanding the effects of mortar placement on the design compressive strength of masonry. Stress-strain graphs were plotted for each test. The mean compressive stress of the HCB from testing is also plotted for reference, allowing direct comparison of the compressive strength of the wallettes. In **Figure 4.9,** the Wallette's utilisation of the block strength was observed. The strain was taken as the average of the cumulative relative difference in both LVDT displacement values over the total height of the wallette sample.

In Wallette testing, failure typically occurs in one or more of the following modes, as seen in **Figure 4.8 :**

(i) Crushing of the blocks under vertical compression due to monolithic behaviour or otherwise.

(ii) Tensile cracking at bed joints due to poor bond or low adhesion of the unit, with cracks propagating from the joints into the blocks.

(iii) Mortar-Block Interface failure due to weak bond, exhibiting zig-zag crack patterns.

(iv) Diagonal cracking resulting from shear due to localised cracking.

(v) Transverse wallette splitting from the side of the wallette due to altered load path.

(vi) Localised crushing due to stress concentrations caused by altered load path.

Failure Mode (i)
Crushed Sample

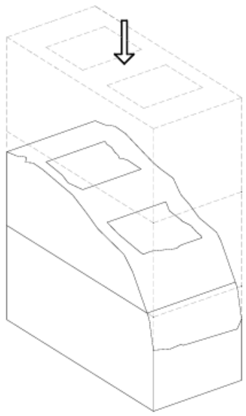

Ref: Fully
Embedded M6(2)

Tensile Cracking (ii)
Crack propagation
from joint

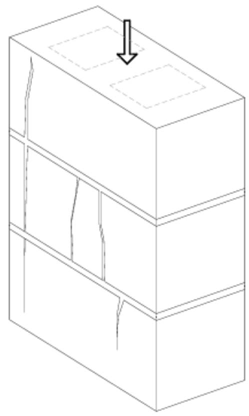

Ref: Fully
Embedded Steel

Mortar-Block Interface (iii)
Shear-Slip Zig-Zag Patterns

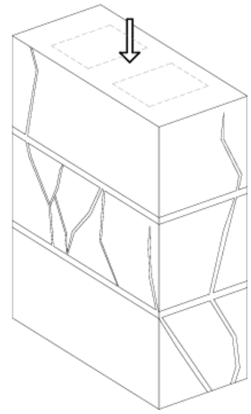

Ref:Shell Bedded
Neoprene

Diagonal Cracking (iv)
Shear - localised weak
points

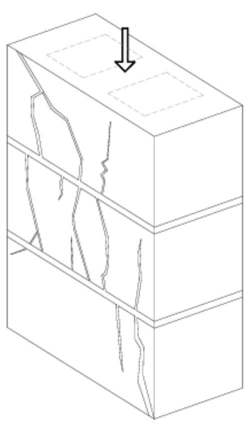

Ref:Transverse Full
M6 (double capped)

Transverse Wall Splitting (v)
Altered load path

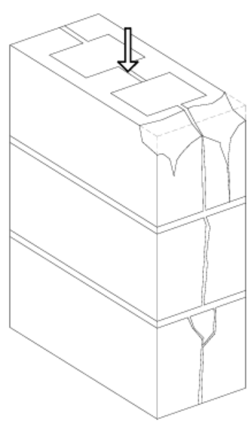

Ref:Shell Bedded
M6 (double capped)

Localised Crushing (vi)
Stress Concentrations

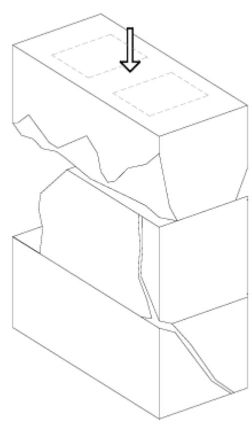

Ref: Steel Shell
Bedded

Figure 4.8: Observed Failure modes of Wallette Samples

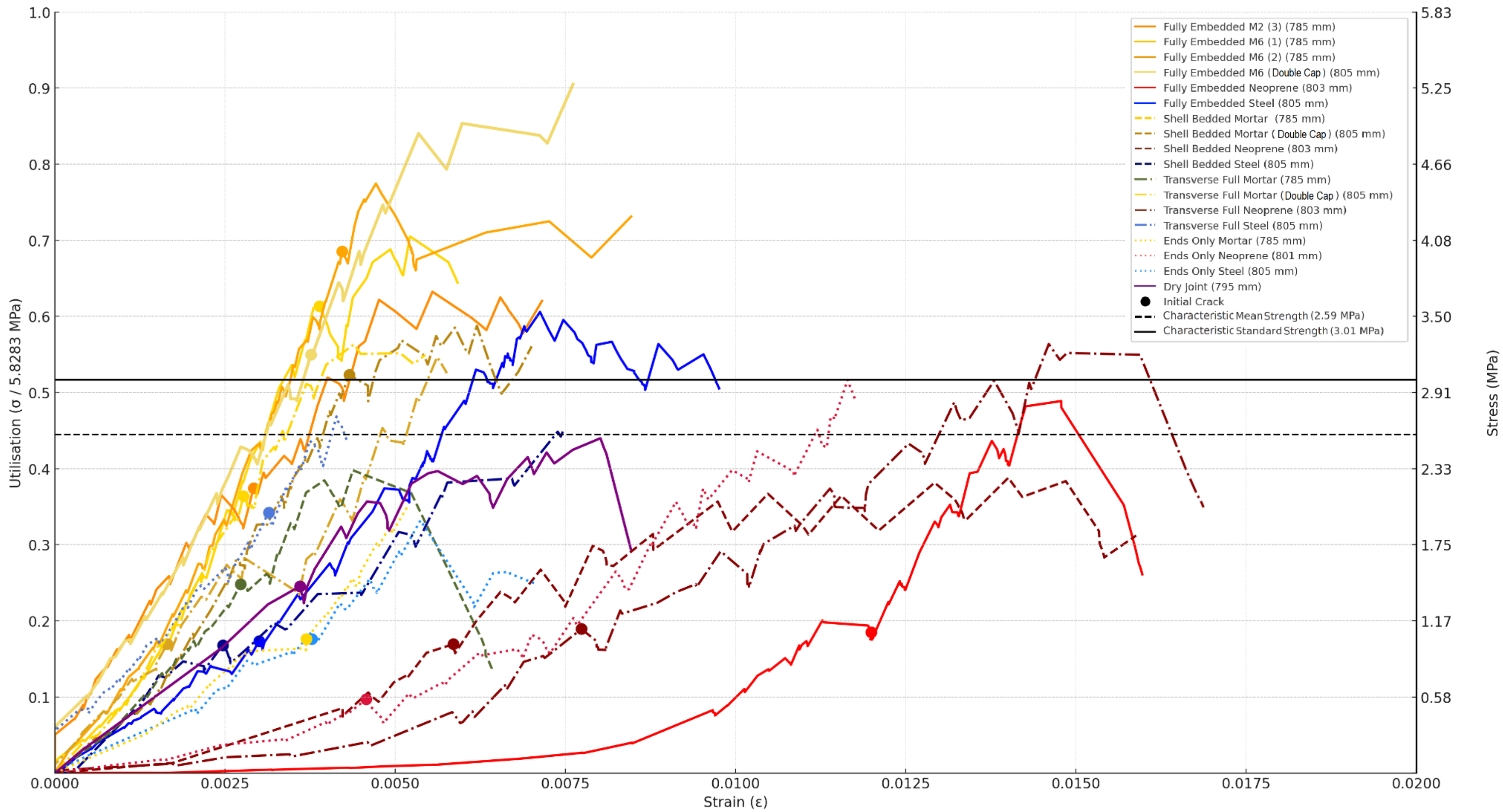

Figure 4.9: All 18 Stress-Strain Test Results

Note: The Characteristic Strengths were calculated using equation 3.1 assuming an M6 mortar. Where α = 0.3, β = 0.7, and K = 0.45. The Standard Characteristic Strength took fb= 7 N/mm2 whilst the Mean

For the comparison of the wallettes to be valid, the gross area was used, including the voids of the HCB, as opposed to the net area, since this changes depending on the placement of mortar, steel or neoprene, as the joint material alters the contact area. Upon comparison, a clear distinction is observed between the mortar and steel cases and the neoprene cases. This distinction between the cases was made because the mortar and steel were stronger than the brick and acted as a hard joint, while the neoprene was weaker and acted as a soft joint.

The initial cracks were also noted by visual observation as dots on the curve, as seen in **Figure 4.9**. This was done to see how the wallettes would behave in terms of serviceability in contrast to their ultimate strength. This is not to say that a crack represents classical serviceability limits like deflection or vibration but rather it serves as an early warning sign of failure. However, it is not a precise benchmark for safe usage, as the initial cracking stresses varied across the tests, with some cases such as the mortar wallettes exhibiting initial cracks at stresses very close to peak stress. The lines are staggered as the load decreases, resulting in cracking.

It is important to note that the stresses plotted in **Figure 4.9** represent unfactored, raw experimental values. Hence, in a real design context, these curves would be considered non-conservative, as loads would be designed based on the allowable design stresses. The "Standard" and "Mean" Characteristic Strength lines plotted represent the expected strengths calculated using an assumed 7 MPa block which is often assumed in practice and a tested 5.828 MPa block which was the actual strength of the block found. Hence it was seen in **Figure 4.9,** that many wallettes exhibited excessive cracking before reaching the standard characteristic strength criteria (fk = 3.01 MPa).

The best-performing wallette is the fully embedded mortar case, which exhibits initial cracking and failure well beyond the characteristic strength specified by EN 1996-1-1:2005. Other cases, such as shell bedding and transverse full cases, barely pass and would have experienced excessive cracking by the point they reached the characteristic strength lines, rendering them useless. The characteristic strength lines reflect that Eurocode design principles use factored i.e. reduced material strength and increased load combinations to ensure safe design, rather than relying directly on raw test capacities. As the fully embedded case performed the best, this emphasises the importance of mortar placement and workmanship on strength and demonstrates the influence of construction quality on meeting design targets. This aligns with the discussion in **Section 4.6**, where it is shown that although many specimens underperform relative to f_k , all the wallettes still meet the design criteria based on the factored design value f_d . This reflects how EN 1996-1-1:2005 uses partial material safety factors to compensate for variability in material properties, execution class and overall quality control.

4.5.1 Fully Embedded Cases

In the neoprene case, pre-compression was accounted for due to self-weight hence, the 5mm joint was reduced to 4mm. It acted as a soft joint until the stress plateaued, at which point the joint was fully compressed, and the bricks then engaged and acted brick to brick. This compression was visually indicated by the flaking of the plaster and its movement outward. This visual flaking is similar to how the plaster compressed on the steel due to its high stiffness and hardness prior to cracking.

The neoprene bedding reached an ultimate stress of 2.85 MPa, which is similar to the dry joint case, which reached 2.56 MPa, as seen in **Figure 4.10.** This similarity in peak stress, further supports the idea that the that the block units began to effectives carry load after the neoprene layer had been compressed. This delayed engagement is in contrast to the steel bedding case which immediately transferred load due to rigidity and reached a maximum stress of 3.53 MPa. The neoprene bedding's initial crack was noted at 1.08 MPa, which was close to the steel bedding's initial crack at 1.01 MPa, as well as the dry joints' at 1.43 MPa.

In contrast, all of the fully embedded mortar cases had initial cracks that occurred at considerably higher stresses ranging from 2.18MPa to 3.99 MPa. This highlights the importance of mortar adhesion with the block i.e. bond strength at the mortar-block interface, which enables the wall to act as a single, unified unit. The neoprene utilised only 48.87% of the HCB strength, indicating the effects of a flexible, soft, deformable "mortar", such as delayed load transfer, reduced compressive capacity, lack of bond i.e. adhesion at the interface and increased deformation. In contrast, the steel case had a higher utilisation at 60.58%, indicating the advantages of a strong, stiff joint, such as efficient load transfer, higher compressive strength and reduced deformation.

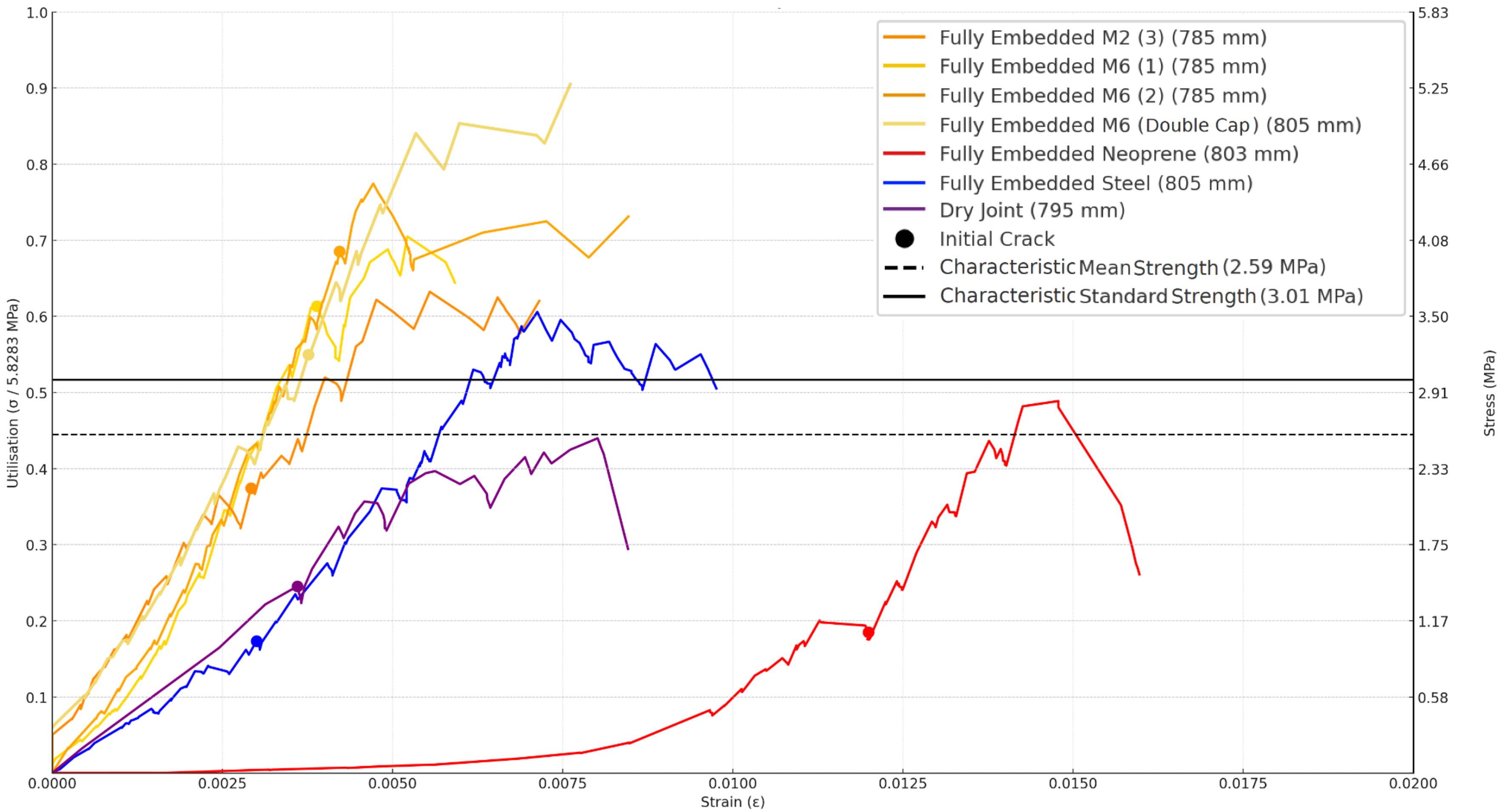

Figure 4.10: All 7 Stress-Strain Fully Embedded Test Results

Note: This test was done 7x; (a) 2x varying the material using steel and neoprene. (b) 2x with an M6 mix cured 2.5-3 days (c) 1x with an M6 mix cured 1 day, equivalent to M2 (d) 1x with an M6 mix cured ≈ 2.5-3 days but with all the bricks double capped to see the effects of reduced adhesion.(e) 1x with a dry joint as a control.

Figure 4.11: Initial Cracking and Failure in Fully Embedded Neoprene Wallette

In terms of failure mode, the neoprene and steel wallettes differed significantly due to their opposing mechanical properties at the joint. In the neoprene case, the cracking progressed into ductile, distributed failure, involving tensile splitting, diagonal shear, and bed joint slipping. This slipping was indicated by zig-zag crack patterns, as seen in **Figure 4.11**, particularly on the right-hand side (RHS) view, in which the cracks followed the joints, indicating relative horizontal displacement between the bricks. This is due to the soft and compressible neoprene, which reduces lateral restraint and allows for slippage due to low friction and minimal confinement. It is important to note that the neoprene cases also exhibited the highest strain values at relatively low stress levels, indicating limited load transfer capacity and lower energy absorption compared to stiffer interfaces. This demonstrated the contrast between stiffness and deformability in hard and soft joints.

Figure 4.12: Initial Cracking and Failure in Fully Embedded Steel Wallette

In contrast, the steel bedding exhibited more brittle failure, as visualised by vertical tensile cracking and localised crushing at the top left-hand side (LHS) corner, this localised crushing occurred close to the peak stress around 3.16 MPa, close to the final 3.53 MPa, as seen in **Figure 4.12.** This is due to steel bedding being a highly stiff, and hard material; hence, when pressed on, the concrete will crush and compress not the steel. It achieved a higher peak strength but showed less ductility due to a more sudden failure. Hence the neoprene showed early, ductile failure as shown by tensile splitting and zig-zag cracking observed in **Figure 4.11** whilst the steel showed localised, brittle failure due to rigid confinement, as seen in **Figure 4.12.** In the mortar cases, it was initially expected that the mortar would perform between the steel, assumed to be infinitely stiff, and the neoprene, being extremely soft; however, it outperformed both in all cases. The mortar wallettes acted as a monolithic unit and didn't crack until close to ultimate stress. The two M6 tests had similar initial cracks of 3.58 MPa and 3.99 MPa, and ultimate stresses of 4.1 MPa at 70.5% utilisation and 4.5 MPa at 77% utilisation of the HCB compressive strength, as seen in **Figure 4.13.**

The Fully Embedded Mortar M6 Double Capped case, had an initial cracking stress of 2.97 MPa with a peak stress of 5.27 MPa at 90.5% utilisation, being the strongest wallette out of the 18 tests. The double capped case was designed to simulate a wallette with reduced adhesion by double-capping all the blocks, as opposed to other mortar cases that only had the top and bottom of the wallette capped and hence had direct adhesion to the brick face. However, this configuration ended up strengthening the unit as a whole by reducing local imperfections at the interface, as well as still having a level of adhesion due to the mortar gripping onto the SIKA 312 capping face but to a lesser extent. The reason for late cracking in the mortar cases was due to uniform load distribution and lack of local failures in the brick due to filling of discontinuities by mortar. The control test i.e. the dry joint case further shows the importance of mortar with early cracking at 1.43 MPa and a much lower ultimate stress of 2.56 MPa at 44% utilisation, as well as having no adhesion due to no mortar present, as seen in **Figure 4.14.** The only mortar case which had early initial cracking at 2.18 MPa was the M2 case with a peak stress of 3.69 MPa at 63% utilisation. This makes sense as it was the weakest mortar with 1 day curing in comparison to other cases which had 3 days of curing.

It is important to note that all the mortar cases reached the characteristic standard strength before cracking ,except for the M2 case. This suggests that Equation 3.1 is valid and conservative when used to estimate characteristic strength for design purposes. This is in contrast to the steel, neoprene and dry joint cases, which exhibited cracking before reaching this point and barely approach the standard characteristic strength. The dry joint not even reaching the mean characteristic strength line which calculated via EN1996-1-1:2005 using equation 3.1 using the actual mean test data of the HCB, as seen in **Figure 4.10**. The neoprene case also failed to meet the standard characteristic strength line, while the steel going exceeded it with excessive cracking. In **Section 4.6**, these results are further evaluated against the design compressive stress f_d , demonstrating that all mortar-configurations pass, confirming the conservative nature of the Eurocode's partial material safety factor.

M6 Mortar (1) @3.6 Mpa   M6 Mortar (2) @4 Mpa   M2 Mortar (3) @2.18 Mpa

Figure 4.13: Initial Cracking of Fully Embedded Mortar Wallettes

Dry Joint @1.43 Mpa   M6 Mortar (double cap)@2.97Mpa

Figure 4.14: Initial Cracking of Fully Embedded Mortar (fully capped) and Dry Joint Wallettes

Confinement is also an important factor to consider as this enhances the load bearing capacity of the mortar. Confinement being the passive lateral restraint that is achieved within the masonry unit and joint during axial compression. While no physical external confinement being applied in the test rig, the pressure from the hydraulic jack and rigidity of the bottom steel beam created internal resistance to lateral expansion, especially in the bed joints. This confinement enhanced the load-bearing capacity of the mortar by limiting lateral strain i.e. Poisson's ratio.

It is also important to note that the plaster did not crack at the joint like it did in the neoprene and steel case. There was little warning of failure, often resulting in a sudden, explosive crushing of the wallette. In fact, in **figures 4.15** and **4.16** there is no image of failure, like in other cases as there was no sample left to photograph. For example, in the double cap case, the top brick remained whole, while the bottom two bricks split in half, showing the high utilisation of the bricks in question. It failed similarly to how a single brick did, via bursting, splitting and crushing of the sides. This is probably as the mortar had a similar hardness and stiffness to the bricks and hence deformed in a similar manner and acted monolithically.

M6 Mortar (1) @4.1 Mpa | M6 Mortar (2) @4.5 Mpa | M2 Mortar (3) @3.69 Mpa

Figure 4.15: Images of Crushed Fully Embedded Mortar Wallettes

In contrast to the dry joint case, in which the whole wall split in half from the sides, such that all the blocks were crushed but did not explode, as the wall was not acting monolithically, as seen in **Figure 4.16**. Additionally, the steel bedding test were overly stiff when compared to the mortar cases, causing brittle failure due to local stresses that led to crushing and edge spalling at the interface, with no adhesion to the interface and non-monolithic behaviour. In the mortar bedding test, at failure the mortar joint sheared off with it sticking to one brick face and being ripped off the other, this indicates that the voids were filled in and were absorbed into the pores. The initial cracks were primarily at the sides; this is dangerous in practice, as a wall could appear uncracked on the outside but internally have a considerable amount of degradation. The exception was the M2 mix, which also showed cracks on the front.

Dry Joint @2.56 Mpa

M6 Mortar (double cap) @5.3Mpa

Figure 4.16: Failure of Fully Embedded Mortar (fully capped) and Dry Joint Wallettes

4.5.2 Shell Bedded Cases

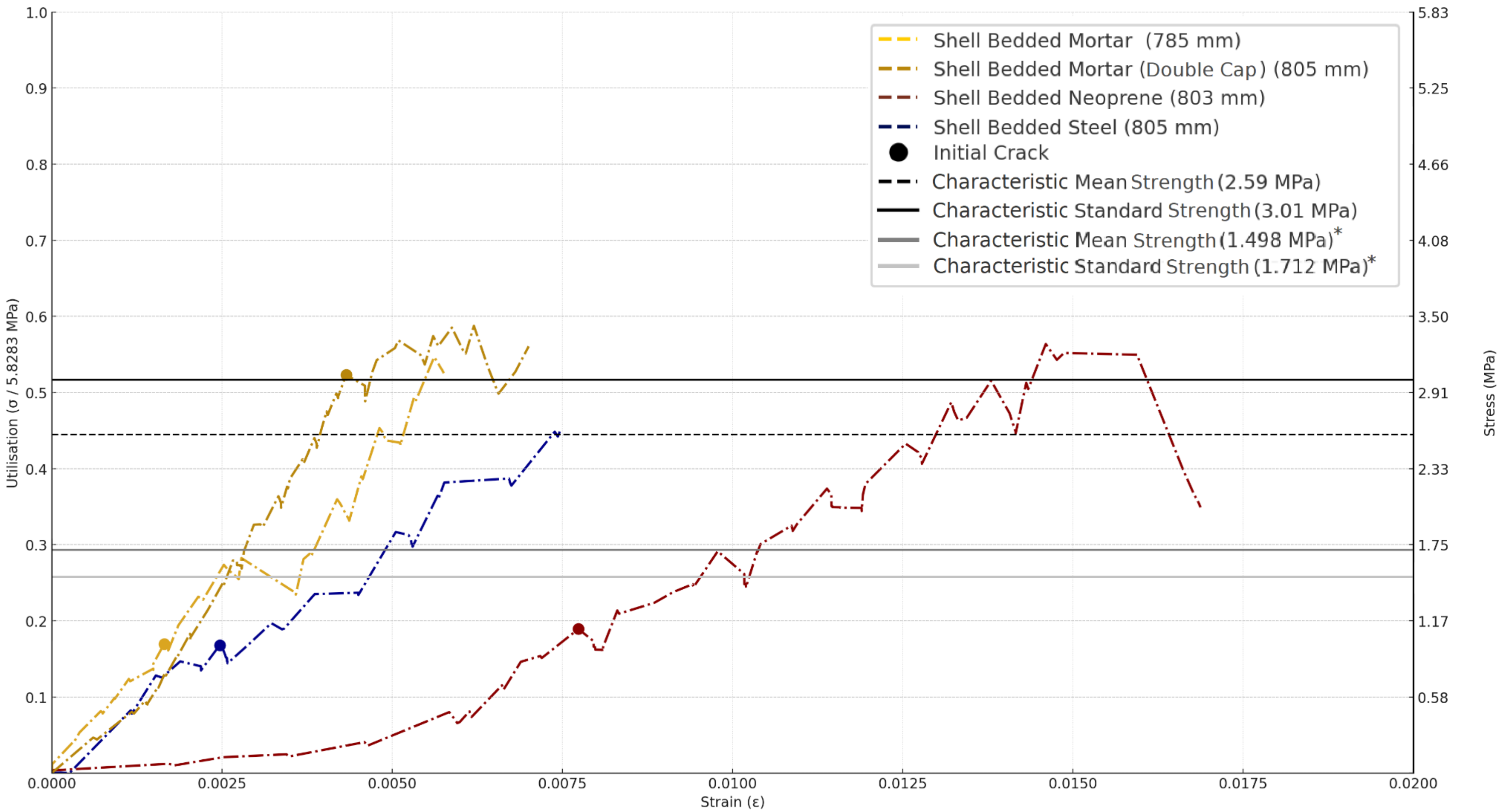

Figure 4.17: All 4 Stress-Strain Shell Bedded Test Results

Note: This test was done 4 times; (a) 2x varying the material using steel and neoprene. (b) 1x with an M6 mix cured ≈ 2.5-3 days (c) 1x with an M6 mix cured ≈ 2.5-3 days but with all bricks double capped to see the effects of reduced adhesion with the block face.

This variation in placement is the most practical as it is used both in the Eurocode and in local construction. Using the modifications as per EN 1996-1-1:2005 Clause 3.6.1.3, the Standard and Mean Characteristic Strengths were calculated via Equation 3.1 using a Halved K factor, based on the g/t ratio, where g = total widths of mortar strips and t = thickness of the unit giving g/t = 106/225 = 0.471. However, as observed in **Figure 4.17** without this modification, the shell bedded cases would barely pass without a partial safety factor (γ_M) and are overall weaker than the Fully Embedded cases, with a drop in strength of 35.11% of the Shell Bedded Fully Capped Wallette, when compared to the Fully Embedded Fully Capped Wallette. It should be noted that all the cases initially cracked at 1 MPa, with the exception of the double-capped case, which cracked at 3 MPa due to fewer local imperfections in the wallette, as the SIKA 312 filled the voids. Again, note that in the mortar bedding test, the cracks initiated at the sides, with the practical implication that if a shell bedding wall starts to split, there would be little warning.

Neoprene @1 Mpa | Steel @1 Mpa | Mortar (M6) @1.1 Mpa | Mortar (Double capped) @3 Mpa

Figure 4.18: Images of Initial Cracking of Shell Bedded Wallettes.

The mortar case failure initiated at the sides and then abruptly bursting at the bottom front face, as seen in **Figures 4.18 and 4.19.** This indicates that, due to the possible arching action of the mortar, a side thrust was induced into the wall face, causing sudden bursting and leading to a wedge-like failure. This is due to internal degradation, discontinuities, and local failures that connect and fail, as seen particularly in **Figure 4.19** in which the lower face of the wallette experienced this wedge failure. This significant change in failure mode indicates that mortar placement controls load path. One should also note that after the release of the hydraulic jack and removal of the spreader beam, the sample was halved, showing the adhesion between the mortar and the unit. This was further strengthened by the fully capped mortar joint tests, which were conducted to mimic less overall monolithic behaviour of the unit, by reducing the bond and adhesion between the mortar and the unit considerably by pre-filling the voids at the interface. These tests enhanced the wallettes by reducing local failures and filling discontinuities, thereby improving load transfer. The Shell Bedded Fully Capped Mortar Wallette achieved a similar strength to the uncapped wallette but still outperformed it by reducing variability and enhancing vertical confinement. As well as having a much later initial crack failing more monolithically at a high stress of 3 MPa in comparison to 1 MPa, as seen in **Figures 4.19** and **4.20.**

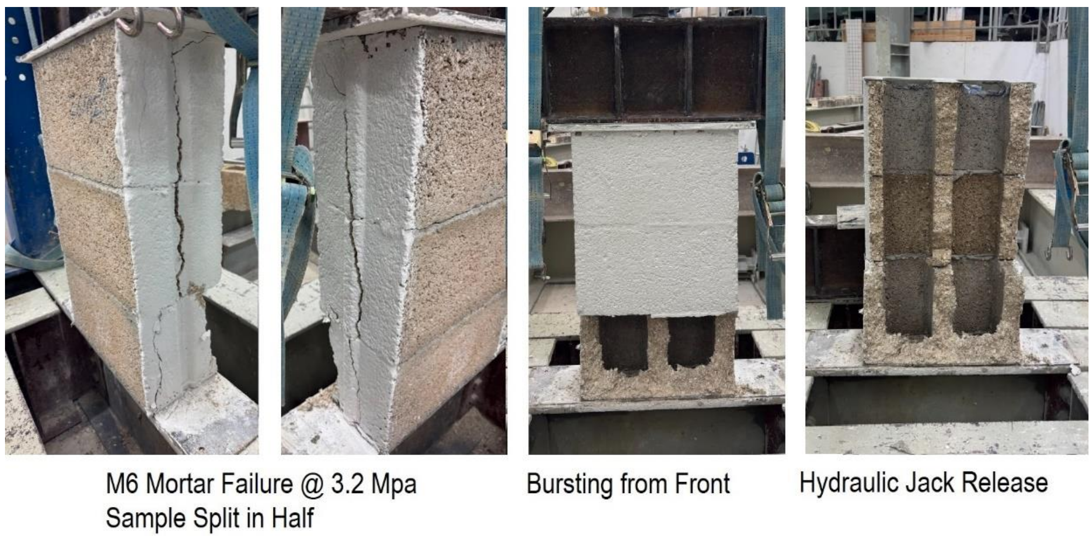

Figure 4.19: Images of M6 Mortar Shell Bedded Wallette Failure

Figure 4.20: Images of Double Capped Mortar Shell Bedded Wallette Failure

In comparison to the neoprene bedding test case, it was observed that it also split in half from the side; however, it did not have a sudden failure like the mortar case. This may have been due to slipping, as indicated by the zig-zag patterns in the failure discontinuities, as seen in **Figure**

4.21. Due to neoprene being soft, it had many fractures and was crushed gradually, with it having been deemed to have failed post excessive cracking, not allowing for further load increases. Hence, this indicates that the mortar controls the "ductility" of the failure, as the mortar bedding tests failed more abruptly compared to the neoprene and steel bedding tests. It is important to note that the neoprene had a similar stress of 3.3 MPa when compared to neoprene bedding tests, showing that the neoprene did compress and the bricks engaged face-to-face.

Neoprene failure @3.3 Mpa LHS RHS

Figure 4.21: Images of Neoprene Shell Bedded Wallette Failure

The steel bedding tests yielded the weakest test results, as the brick itself was crushed in compression, while the steel did not compress, resulting in significantly less strain. This is due to the concentrated stress it experienced from the side thrust and arching action, which again caused fracture and wedge failure, however, with higher localised stresses due to the stiffness of the steel as it was being pushed into the brick in compression. As observed from the localised crushing experienced around the steel joints in the wallette, shown in **figure 4.22.**

Steel failure @ 2.6 Mpa LHS RHS

Figure 4.22: Images of Steel Shell Bedded Wallette Failure

4.5.3 Transverse Full Cases

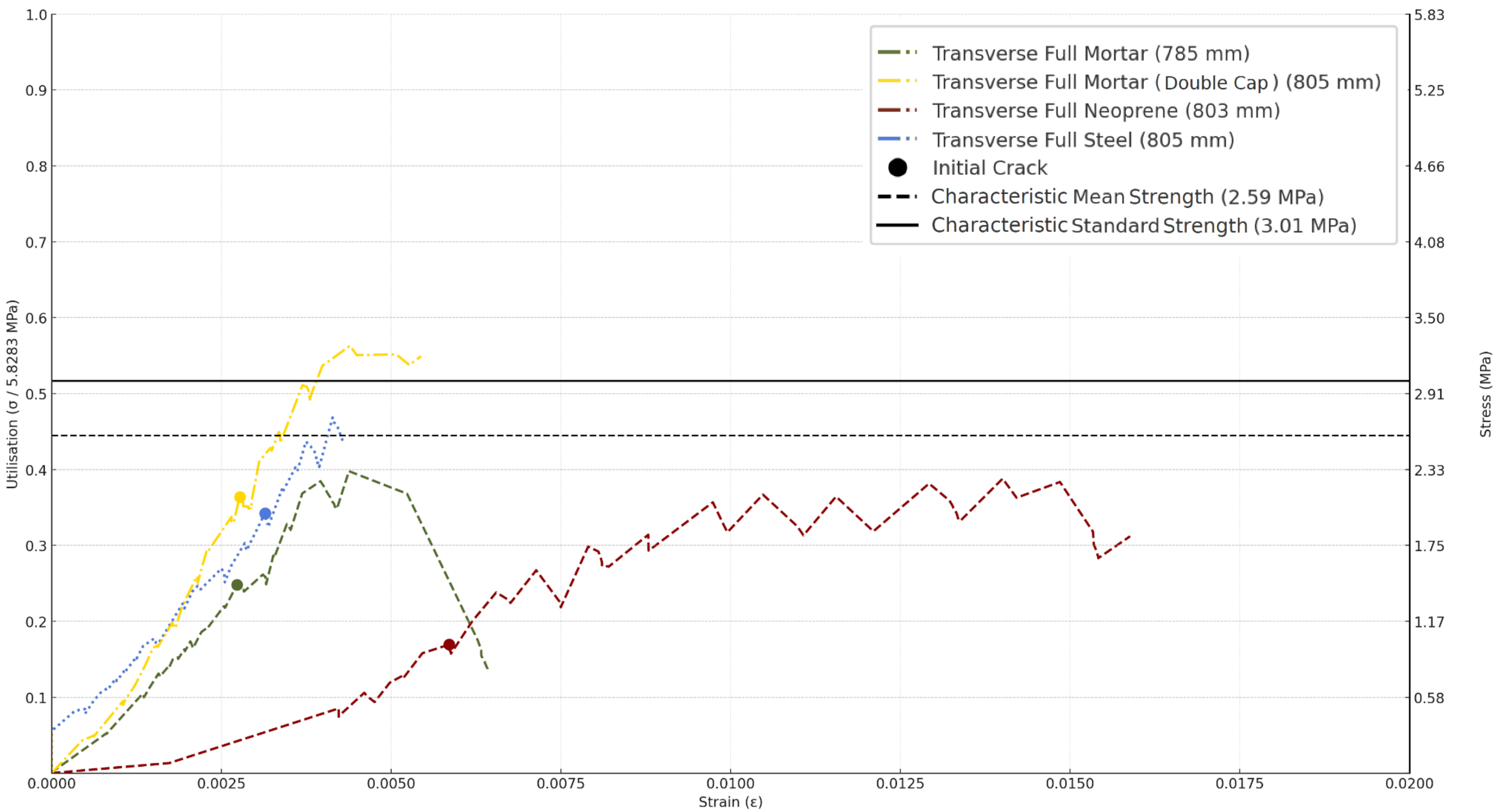

Figure 4.23: All 4 Stress-Strain Transverse Full Test Results

Note: This test was done 4 times; (a) 2x varying the material using steel and neoprene. (b) 1x with an M6 mix cured ≈ 2.5-3 days (c) 1x with an M6 mix cured ≈ 2.5-3 days but with all bricks double capped to see the effects of reduced adhesion with the face of the brick.

The initial cracks primarily occurred at the sides, except for the steel bedding tests, which exhibited a vertical crack along the front face, possibly indicating tension in the mid-span region between each steel plate, as seen in **Figures 4.24** and **4.25.** However, it is important to note that no tensile strain measurements were taken from this hence the crack pattern may also be influenced by other factors such as stress concentrations. The mortar bedding tests revealed a crack at the bottom central mortar joint, indicating that the joint had begun to crush and was being compressed into the bottom brick. One should note that, once again, the double-capped mortar bedding tests cracked later than the uncapped case, showing that having fewer initial discontinuities in the block leads to a higher compressive strength. In this case, the SIKA 312 capping overall strengthens the wallette, as seen in other cases. The practical implications of early cracking at the sides are that one would not notice this on-site, as opposed to front cracks, which are visually more evident.

Neoprene LHS @1Mpa Neoprene RHS Steel @2Mpa

Figure 4.24: Initial Cracking of Neoprene and Steel Transverse Full Wallettes

M6 LHS @1.45 Mpa M6 Front M6 (double cap)@2.12 Mpa

Figure 4.25: Initial Cracking of Mortar Transverse Full Wallettes

In the neoprene bedding tests pre-compression of the bedding joint was accounted for due to self-weight of the overlying block hence the 5mm joint was reduced to circa 4mm. The neoprene wallette experienced complete crushing of the left side at the joint, as seen in **Figure 4.26.** In comparison to other neoprene bedding tests, it reached a lower stress of 2.26 MPa. However, this could be attributed more to the variation in the quality of the bricks, as the neoprene was already fully compressed. Failure was deemed to have occurred at the point at which the block's fractures prevented it from supporting further load. It is possible that the HCB blocks contained internal defects such as voids, honeycombing, or weak zones caused by poor compaction or segregation during casting. These imperfections whilst not externally visible may have acted as stress concentrations, which allowed for the quicker creation of fractures and ultimate failure. As the unilateral crushing observed suggests, the load path was altered due to the transverse strips of neoprene but also potentially the localised stress concentrations, which caused one side of the unit to fail prematurely.

Figure 4.26: Images of Neoprene Full Wallette Failure

In the steel bedding tests, it reached a higher stress of 2.73 MPa when compared to the neoprene bedding test but less than the mortar case. The steel wallette outperformed the neoprene wallette likely due to a high-stress concentration at the bedding joint, as well as at the left-hand side, as observed in **Figure 4.27**, where large fractures propagate from the joint where the steel is placed. This indicates that, despite its higher stiffness, steel bedding lacks the adhesive bonding that mortar induces, leading to localised stress concentrations and a less effective stress distribution.

Steel Failure @ 2.73 Mpa LHS

Figure 4.27: Images of Steel Full Wallette Failure

In the mortar transverse sides full tests, when comparing it to its counterpart with only ends, as expected, the “span” was essentially halved due to central support and hence outperformed it, reaching a stress of 2.32 MPa in comparison to 2.04 MPa. As a result, tensile stresses are minimised and compressive forces are more uniformly distributed, leading to a 13.2% relative increase in load-bearing capacity, when compared to the Ends Only Mortar Wallette.

The improved load transfer and shortened “span” may have contributed to a better distribution of strain. However, both the capped and the uncapped transverse cases exhibited higher maximum strains of 0.0054 and 0.0064 respectively, in comparison to the ends only case at 0.0052. This suggests that while the altered load path reduced localised deformation and delayed cracking, it did not lead to lower overall strain at failure. It should be noted that this is based off three tests and more samples would be needed to reliably assess the deformation behaviour of the wallettes.

M6 Failure @ 2.32 Mpa LHS

Figure 4.28: Images of M6 Mortar Transverse Full Wallette Failure

When testing the double capped wallette with poor adhesion i.e. with less bond due to the voids are filled so the mortar grips less at the interface, all three blocks experienced a crushing failure with tensile cracks in between the joints. This failure is due to fractures propagating at the joint interface, not allowing the wallet to take more load. One should note that both the double-capped and uncapped mortar wallets followed similar cracking patterns. The idea behind this setup was to promote vertical load transfer through the centreline of the unit, which should reduce flexure. However, it still allowed for diagonal splitting due to stress distribution at the supports, indicating shear and tensile failure mechanisms, as observed in **Figures 4.28 and 4.29**

M6 (double cap) Failure @ 3.28 Mpa LHS RHS

Figure 4.29: Images of M6 Mortar Transverse Full (double capped) Wallette Failure

4.5.4 Ends Only Cases

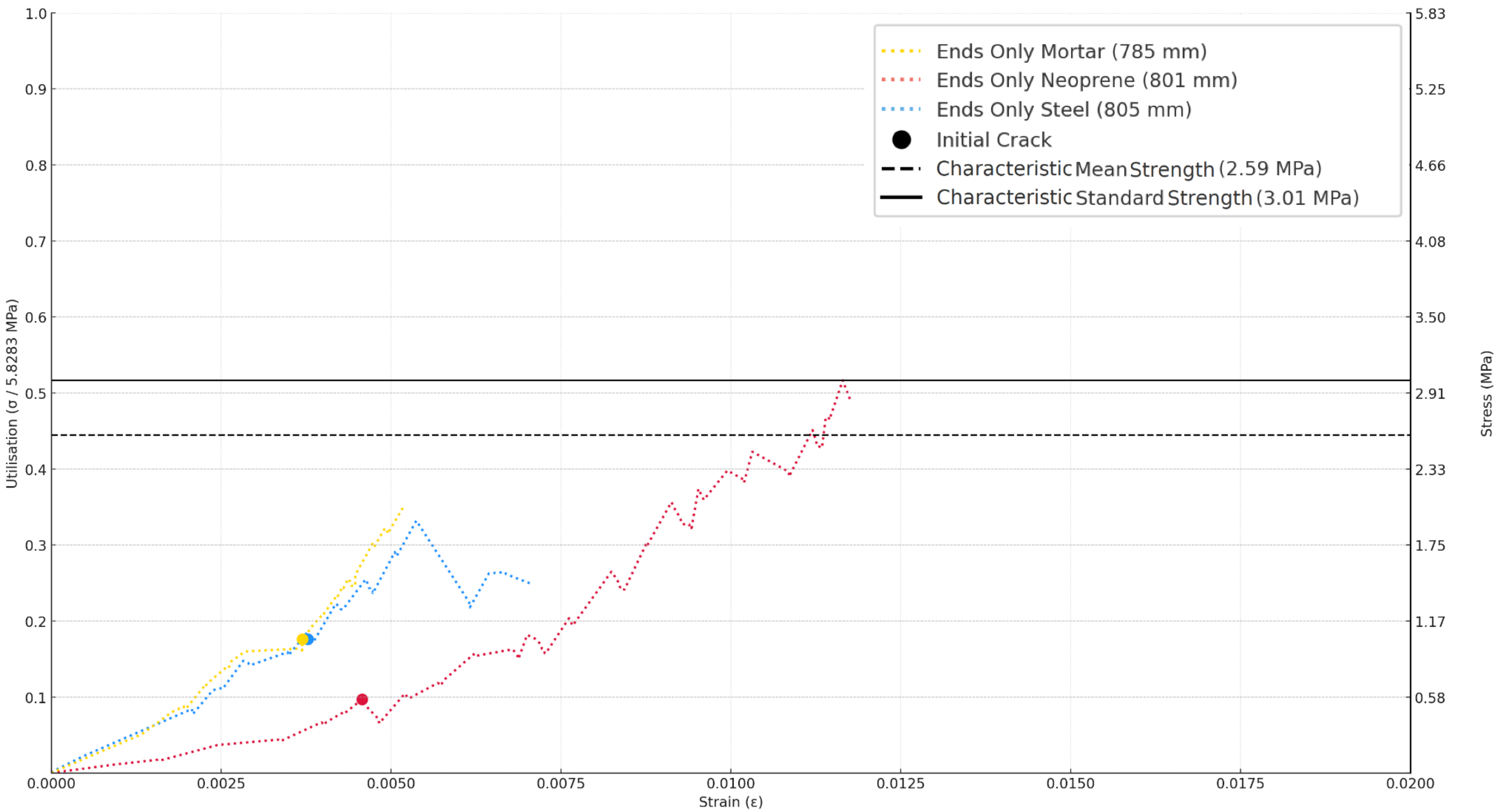

Figure 4.30: All 3 Stress-Strain Ends Only Test Results

Note: This test was done 3 times; (a) 2x varying the material using steel and neoprene. (b) 1x with an M6 mix cured ≈ 2.5-3 days. The double capped test was not done due to time constraints.

The Ends only test was designed to induce flexure in the brick by making each brick “simply supported” by applying material only at the sides. The top block behaves as a short-span beam bending with tension at the midspan and compression at the supports. This led to all the bricks initiating cracking at the ends, where the material was placed, propagating upwards from the joint, inducing tension in the “span,” i.e., the joint between each “support.” The steel and mortar bedded wallettes were the weakest, showing the importance of bedding placement in masonry and the effects of the load path. The neoprene bedded test is only stronger due to the joint compressing and allowing for brick-to-brick face engagement, as if the material were not there.

The neoprene bedded test experienced pre-compression due to self-weight; hence, from a 5mm joint, it reduced to 3mm. The wallette failed along the cracks caused by the altered load path, with the initial crack having occurred at the central brick, as seen in **Figure 4.31**, propagating into the upper brick at the sides and into the lower brick at the front. All three blocks were cracking along the same load path line at the joint due to a stress concentration caused by the neoprene, as seen in **Figure 4.32.** Despite this, it still reached a similar ultimate stress of 3 MPa when compared to neoprene bedded test.

Neoprene@0.6 Mpa | Steel@1.08 Mpa | Mortar (M6)@1.03 Mpa

Figure 4.31: Images of Initial Cracking of All Ends only Wallette Cases

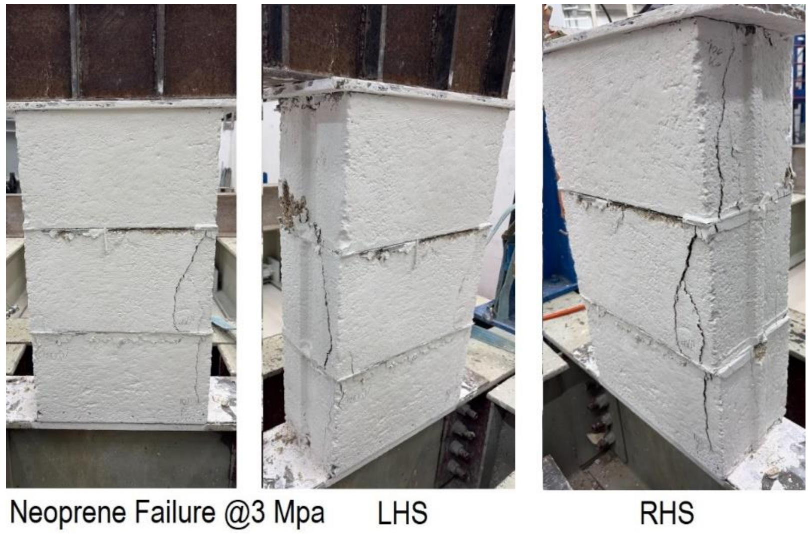

Figure 4.32: Images of Neoprene Ends Only Wallette Failure

The steel ends only test demonstrated the importance of load path, as the ultimate stress was 1.93 MPa, making it the weakest out of 18 tests. Due to high-stress concentrations, the right side of the wallette broke off at the joint, as the steel was pressed into the hollow concrete blocks, as seen in **Figure 4.33.** The mortar bedded test outperformed the steel by a small margin, reaching a peak stress of 2.04 MPa. This is due little mortar in the joint, hence less adhesion occurred at the interface causing little monolithic behaviour in the wallette. Therefore, it acted like a hard joint, similar to steel, reaching a higher stress, as when the mortar is pressed into the block, it still has a similar stiffness. However, as the steel bedded joint induces no monolithic behaviour in the wallette, it induces high stress concentrations acting rigidly; hence, the failure mode observed was local failure, as opposed to global crushing or flexural splitting, as seen in **Figure 4.34.**

Figure 4.33: Images of Steel Ends Only Wallette Failure

Figure 4.34: Images of Mortar Ends Only Wallette Failure

Overall, the end-only cases experienced arching action from support to support, which led to tension in the brick and the joint. Hence, the top brick experiences crushing due to joint failure as it is pushed into the brick and fractures at the joint, causing the unsupported brick to go into tension. The tensile cracking of the unsupported midspan, in combination with edge crushing at the supports, highlights how poor workmanship and improper placement alter the load path and induce new modes of failure. It is important to note that the ends only mortar, showing the lowest stiffness out of the mortar cases , with an Elastic Composite modulus of 339.41 MPa, which is extrapolated from the gradient of a linear cut of the curve, as seen in **Table 4.2.** Whilst giving the highest strain with relatively low stresses indicating poor load transfer capacity and lower energy absorption.

It is essential to note that the elastic modulus is a composite value, as it encompasses the stiffness of both the mortar joints and the blocks. The highest modulus is that of the fully bedded mortar Wallette, with a modulus of 907.41 MPa, which outperformed this wallette in all aspects. It is essential to note that due to the failure of one side of the wallette, the spreader beam rotated to one end, causing one LVDT to be pressed up and the other down. Consequently, such values were disregarded as they would not be consistent with the prior data. Hence, it can be said that overall, the most brittle failure highlights the importance of proper joint continuity and bedding in terms of strength and failure mode.

Test	$\sigma 1$ (MPa)	$\varepsilon 1$	$\sigma 2$ (MPa)	$\varepsilon 2$
Fully Embedded M6 (Double Capped)	0	0	4.8475	0.005342086
Fully Embedded M6 1	0	0	3.084	0.003501
Fully Embedded M6 2	0	0	3.3976	0.003887
Transverse Full Mortar (Double Capped)	0	0	2.474	0.003239
Fully Embedded M2 (3)	0	0	2.8106	0.003857
Shell Bedded Mortar (Double Capped)	0	0	2.5648	0.003856
Transverse Full Steel	0	0	1.9954	0.003139
Transverse Full Mortar	0	0	1.6704	0.003263
Shell Bedded Mortar	0	0	2.271	0.004546
Fully Embedded Neoprene	0.4398	0.009697	2.0543	0.013151
Fully Embedded Steel	0	0	2.6459	0.005741
Dry Joint	0	0	1.4303	0.0036
Shell Bedded Steel	0	0	1.8452	0.005051
Ends Only mortar	0	0	1.5196	0.004473
Transverse Full Neoprene	0.4321	0.004228	1.7012	0.008051
Ends Only Steel	0	0	1.4524	0.004654
Ends Only Neoprene	0.4617	0.004324	2.2526	0.010177
Shell Bedded Neoprene	0.6379	0.006634	2.457	0.012724

Table 4.2: All 18 Stress-Strain Curve Composite Elastic Moduli

4.6. The effects of the partial safety factor - γ_M

As per clause 2.4 of EN 1996-1:2005, the characteristic strength of the masonry f_k found using equation 3.1 can be further verified through a partial factor method. A similar clause is found in MSA EN 1996-3:2006,-clause 2.3 which presents a simplified version of the same table.

$$f_d = \frac{f_k}{\gamma_M}$$

Where f_d = design compressive strength,

f_k = characteristic compressive strength, γ_M = material safety factor

Equation 4a - Eurocode 6, EN 1996-1-1:2005, Clause 2.4

For ultimate limit states via clause 2.4.3 of EN 1996-1-1:2004, as hollow concrete blocks are Category II units, and using an M6 general-purpose mortar, using a Class 4 execution control is adopted. Accordingly, the chosen partial safety factor γ_M value is 2.7. The classes in question do not reflect workmanship alone but rather the overall level of material quality assurance, site supervision and construction control i.e. general quality control.

Hence the classes represent execution control, with Class 1 representing the highest confidence, associated with factory-controlled conditions and rigorous testing. While Class 5 represents the lowest level of control. Given the observed variability in local site practices, Class 4 was considered suitable to reflect the relatively low confidence in supervision and construction quality.

The safety factor approach indirectly accounts for variability in construction, including poor workmanship and material inconsistency commonly observed locally. When γ_M is applied to the characteristic strength f_k, the values of 3.01 MPa (standard 7MPa block) and 2.59 MPa (tested mean of HCB 5.828MPa) are reduced to 1.11 MPa and 0.96 MPa respectively.

Only the mortar wallette cases were evaluated against the design compressive strength f_d as they represent realistic construction cases. The steel, neoprene and dry joint cases served as comparative extremes to study joint effects and do not reflect applicable structural designs under Eurocode 6.

According to Clause 6.1.2.1 of EN 1996-1-1:2005, the design vertical resistance of a masonry wall (N_{Rd}) is given by:

$$N_{Rd}=\Phi \cdot f_d \cdot t$$ **Equation 6.2 - Eurocode 6, EN 1996-1-1:2005, Clause 6.1.2.1**

Where t = thickness of wall , Φ = Slenderness Reduction factor, f_d = design compressive strength,

However, this equation is intended for full-height structural masonry walls where instability and buckling are considered. In this study, the wallette samples had a very low height-to-thickness ratio ranging from 3.49 to 3.58 and are therefore considered to be stocky elements not susceptible to slenderness effects. For this reason, the performance of said wallettes was assessed directly against the design compressive stress f_d , allowing the influence of mortar strength, joint configuration and workmanship without the influence of geometric stability effects.

As seen in **figure 4.35,** all the wallette cases satisfy the design criteria under these reduced values with respect to ultimate limit state. However, in terms of serviceability some cases such as the ends, transverse and shell bedded cases exhibit cracking within or close to these stresses indicating that they may not satisfy serviceability requirements. This safety factor method overall conveys the conservative approach Eurocode 6 takes with respect to masonry design, where large partial safety factors are taken to account for variations in block work and mortar performance.

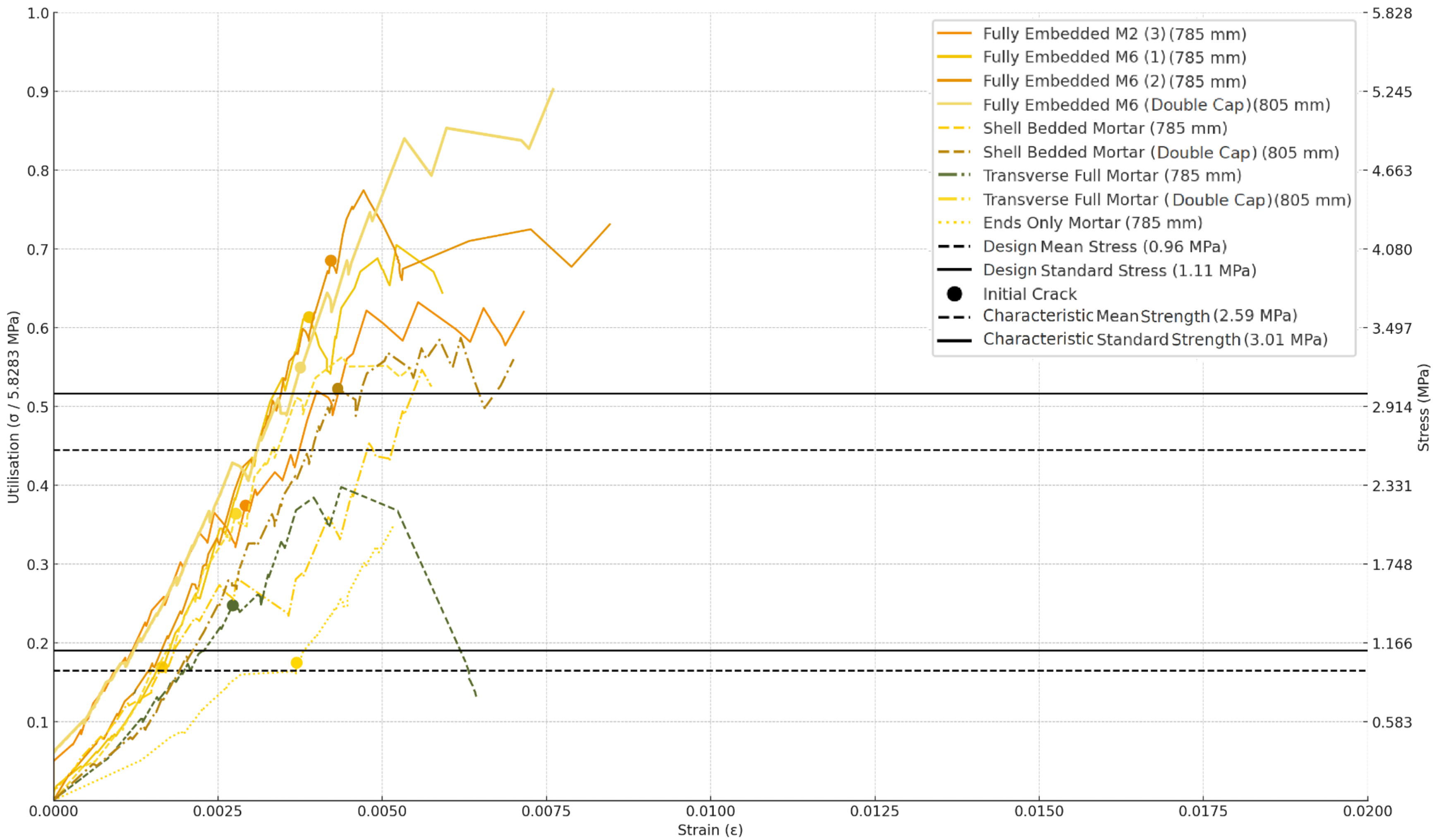

Figure 4.35: All 9 Stress-Strain Mortar Test Results

5. Conclusion

5.1 Summary of Findings

This research focused on the effects of mortar placement on masonry compressive strength. Design codes, such as EN 1996-1:2005, do not directly account for the influence of workmanship on failure modes in design but compensate for it with high material partial safety factors. To explore this gap, the effects on compressive strength, based on mortar stiffness, strength and placement, which mimics poor workmanship, were investigated by constructing several three-course high wallettes. Each wallette, being tested until failure, was loaded at intervals of 50 kN/min, with load and displacement being measured.

In total, four different cases were investigated:

(1) Fully Embedded – Mortar placed fully on the bed joint, allowing for monolithic behaviour and full load transfer.

(2) Shell Bedded – Mortar placed only on the longitudinal sides of the unit, reducing contract area and altering load path.

(3) Transverse Full – Mortar placed only on the transverse sides of the unit, reducing contact area and altering load path.

(4) Ends only – Mortar placed only at the end sides of the unit, attempting to induce flexure in the block unit.

The tests carried out focused on obtaining the values of stress and strain measured over the entire wallette. Each test result was compared against the mean compressive stress of the HCB block (the control block) and also to design limits recommended in EN 1996-1:2005, in order to evaluate strength reduction in compressive strength due to mortar joint strength and workmanship via placement. First, the wallettes were compared to the characteristic strengths (f_k) as a baseline threshold and later compared to the allowable design stresses (f_d), in order to demonstrate the application of the design provisions in EN 1996-1-1:2005.

An observational discussion, i.e. a discussion that is structured to reflect data obtained during testing as well as visual observations, was carried out regarding the compressive load at which initial cracking occurred. This was considered to be the serviceability limit of the wallette. In addition to this, the ultimate compressive load-carrying capacity was also noted. It should be noted that in many cases, excessive cracking of the HCB was evident, with immediate failure occurring.

The structural performance of the tested wallette mortar configurations, relative to the compressive strength of the HCB, is presented in **Table 5.1** and **Table 5.2**. The efficiency is the ratio of the ultimate compressive stress achieved by the wallette to the HCB peak stress of the unit. The results revealed a broad spectrum, ranging from 33% to 90%. The highest-performing case being the Fully Embedded M6 Mortar (Double Capped) case, with the weakest being the Ends Only Steel case.

Test	Peak Stress (Mpa)	Effeciency
Hollow Concrete Block Unit	5.828	100%
Fully Embedded M6 (Double Cap)	5.27	90%
Fully Embedded M6 (2)	4.51	77%
Fully Embedded M6 (1)	4.11	71%
Fully Embedded M2	3.69	63%
Shell Bedded M6 (Double Cap)	3.42	59%
Tranverse Full M6 (Double Cap)	3.28	56%
Shell Bedded M6	3.19	55%
Transverse Full M6	2.32	40%
Ends Only M6	2.06	35%

Table 5.1 Efficiency of Mortar Joint Wallettes w.r.t HCB mean compressive strength

Test	Peak Stress (Mpa)	Effeciency
Hollow Concrete Block Unit	5.828	100%
Fully Embedded Steel	3.53	61%
Shell Bedded Neoprene	3.29	56%
Ends Only Neoprene	3.01	52%
Fully Embedded Neoprene	2.85	49%
Transverse Full Steel	2.73	47%
Shell Bedded Steel	2.61	45%
Dry Joint	2.56	44%
Transverse Full Neoprene	2.26	39%
Ends Only Steel	1.93	33%

Table 5.2 Efficiency of Material Joint Wallettes w.r.t HCB mean compressive strength

5.2. Effects of Workmanship and Placement

It was observed that the fully embedded mortar case was the most efficient in terms of least displacement, with the greatest ultimate mode. This indicates that mortar placement is crucial and significantly influences the ductility and failure mode of masonry, as it controls both the load path and the monolithic behaviour of the masonry construction i.e. the adhesion at the joint interface. The effects of a strong mortar i.e. stronger than the block unit strength in comparison to a soft joint such as neoprene, lead to more cracking in the wallette and alter the failure mode from brittle, monolithic block failure to ductile, joint-driven failure involving slip and shear, changing the mode of failure altogether. One should also note that the initial cracks indicated the effects that the mortar placement and strength have on the serviceability load. As weaker wallettes experienced initial cracking at around 1 MPa, at a displacement of 1 mm per joint, this implies that in normal construction practices of 11 courses of HCB per floor, the height per storey would be approximately 11 mm. This is in contrast to the fully embedded case, which experienced late initial cracking for the same displacement. This shows the importance of proper workmanship and placement in terms of serviceability as opposed to just strength. Serviceability failure will always precede ultimate structural failure, providing important telltales such as cracking of wall finishes.

5.3 Eurocode 6 Design Recommendations

Throughout the study, the test compressive strengths were compared to the design compressive strengths derived from EN 1996-1:2005, Equation 3.1. It was observed that EN 1996-1:2005 primarily relies on block unit compressive strength (f_b) rather than mortar compressive strength (f_m), as indicated by the exponents in Equation 3.1 of which gives f_b greater influence. Furthermore, EN 1996-11-1 does not explicitly account for workmanship-related effects, such as incomplete joint filling, poor adhesion or inconsistent mortar placement. It only allows a variation in the case of shell bedding, through a reduction in the K factor, which partially accounts for the reduced area but does not cover other practical placement variations.

As observed in **Figures 4.8** and **4.9** that the code appears conservative for fully embedded mortar and shell bedded cases. However, other configuration such as transverse full and ends only mortar placements performed significantly worse in comparison. This is understandable, as EN 1996-1-1 is not designed to incorporate non-standard joint layouts or variability induced by poor workmanship. Instead, the code compensates for such variability through conservative material partial safety factors γ_M which reduces the required design strength considerably allowing for all the tested wallettes to pass the ultimate limit state check, as seen in **Figure 4.35.** This indicates that the code indirectly compensates for unknown workmanship variability through strength reduction rather than explicit modelling. However, based on the wallette test results obtained in this study, a preliminary correction factor could be proposed to be applied to the characteristic strength f_k , prior to the γ_M based reduction. This could allow for more precise estimate of design compressive strength of masonry while ensuring safety and reliability. It should be noted that the data set of this dissertation is limited. Further testing would be required to establish a statistically meaningful average before any design guidance can be validated. For example:

- The Ends Only Mortar ends case achieved 35% of the strength of the fully embedded case.
- The Transverse Full case achieved 40% and 56% when double capped.

Therefore, when using non-standard joint configurations similar to these, the design compressive strength (f_k) could be adjusted by applying a correction factor ranging from 0.35 to 0.56, depending on placement used with the Fully Embedded acting as a baseline of 1.0.

In simple terms; **$f_{k,\text{ reduced}} = f_k \times$ correction factor (equation 5.1)**

Additionally, this study highlighted the issue of overestimating the block unit strength. Engineers locally often assume a Hollow Concrete Block of 7MPa; however, testing revealed a mean compressive strength of 5.828 MPa with a coefficient of variance (C.O.V) of 11.79%, leading to a 14% reduction in characteristic strength relative to the assumed value. In conclusion by combining proposed workmanship-related correction factor with verified tested material properties would yield a more realistic and safer basis for masonry design. However, given the application of a material safety factor, Eurocode 6 introduces a lot of allowances for poor workmanship and material variability terms of the block unit and mortar.

5.4 Effects of Joint Strength and Stiffness

It can be said that this study highlights that mortar placement not only acts as a levelling filler but also significantly influences the structural behaviour of masonry, affecting both load path and failure mode. This supports the notion that masonry should be designed as a composite system, rather than primarily considering block strength. EN 1996-1-1:2005 recognises composite behaviour through equation 3.1 where f_k is influenced by both unit and mortar strength, these equations however assume good workmanship and isotropic joint properties. The experimental data of this dissertation shows that mortar placement can reduce strength by 65% which is not currently reflected in the code. Hence this research demonstrates the need to account for both material properties and workmanship in masonry design. The steel, neoprene and dry Joint cases were included in this study to simulate extreme cases of joint stiffness. The steel was the stiffest and hardest joint material; tests with this configuration failed in an abrupt, brittle manner but still exhibited greater levels of strain than the mortar joints despite failing at a lower compressive strength. Neoprene having the softest and weakest joint, failed in a very slow ductile manner, as well as experiencing the most strain.

On average, across all four full mortar wallettes tested, an average utilisation of 75.4% of the HCB unit strength was achieved. These tests were prioritised and repeated as the full embedment case represents the standard recommended practice and served as a control of the data set for comparison. Hence establishing the performance of fully embedded joints was essential in the evaluation of variation in mortar placements and their effect on strength. The full embedment cased outperformed the shell bedding mortar cases by 18.4%, the transverse full cases by 27.4% and ends only by 40.3%, when compared to the average of the 4 fully embedded wallettes. This difference in performance highlights the influence of mortar placement on the structural behaviour and performance of masonry construction, the need for good workmanship and the importance of adhering to standards in construction.

5.5 Recommendations for Further Research

This research study was exploratory; therefore, it is recommended that further testing be conducted in the future to establish the standard deviation (S.D.) and the coefficient of variation (C.O.V.) for each mortar configuration. It is also worth noting that the quality of the HCB unit is a crucial factor, and it would be beneficial to conduct a national study using HCB units obtained from multiple manufacturers.

5.5.1 Larger-Scale Wall Testing

It would be more meaningful to create a larger wall sample with head joints to achieve a more realistic setup, as masonry is constructed staggered rather than vertically. Hence, this approach would yield more practical results, revealing better insights into masonry construction performance. In addition to the rate of loading, on-site loading is done gradually and over time, as opposed to the rapid rate tested in this dissertation. This gradual application of the load allows for time-dependent effects such as creep, stress redistribution and delayed cracking to be observed. Hence, if the wall were tested over days or weeks instead of minutes, it would more accurately reflect actual site conditions and provide a better understanding of masonry performance under realistic long term service loads

5.5.2 Computational Model using Finite Element Analysis Software

Young's modulus of elasticity as a smeared value for the brick-and-mortar wallettes tests has been found. However, it would be meaningful to find the Young's modulus of elasticity of the mortar and the single HCB unit, which then can be used to use finite element analysis (FEA) software to calibrate the tests carried out in this study and to carry out then further exploratory studies of the behaviour of mortar placement in walls.

5.5.3 Other workmanship alternations

Further research should be conducted to investigate common site modifications on load-bearing masonry walls other than mortar placement and block quality, such as horizontal and vertical pipe chases for water or electrical services. Further studies may lead to insights into localised stress concentrations, altered load paths and crack propagation. EN 1996-1:2005 specifies limits on chasing, for example for units with a thickness of 225 mm, the max vertical chase depth is 30mm and the max horizontal chase is 10 mm for chases of length less than 1250mm, but these rules are often ignored on site. In practice the cases are usually deeper as well as longer than 1250mm, which may severely reduce the structural integrity of the masonry wall, creating local weaknesses.

5.5.4 Lateral Loading

It would be relevant to set up a similar system, but with the addition of a lateral force, to see how walls are affected by mortar placement in terms of flexure. This would be meaningful in order to see the effects of such variation in mortar placement.

Bibliography

1. *Abaza, O. A., & Abu Salameh, A. (2003). 'The effect of capping condition on the compressive strength of concrete hollow blocks' , An-Najah University Journal for Research , 17(1).* https://doi.org/10.35552/anujr.a.17.1.646
2. *BS EN 772–1 (2011)." Methods for test for Masonry Units Part1: Determination of Compressive Strength", BSI Standards Publication*
3. *BS EN 771-3:(2011+A1:2015), "Specification for masonry units, Part 3: Aggregate Concrete Masonry Units (Dense and lightweight aggregates)", BSI Standards Publication*
4. *BS EN 771-5:(2011+A1:2015), "Specification for masonry units, Part 5: Manufactured stone masonry units", BSI Standards Publication*
5. *BS EN 998-2:(2016), Specification for mortar for masonry, BSI Standards Publication.*
6. *BS EN 1015–11:(1999), Methods of Test for Mortar for Masonry – Part 11: Determination of flexural and compressive strength of hardened mortar, BSI Standards Publication*
7. *BS EN 1052–1:(1999), Methods of Test for Masonry – Part 1: Determination of Compressive Strength, BSI Standards Publication*
8. *BS EN 1052–2:(1999), Methods of Test for Masonry – Part 2: Bulk sampling of mortars and preparation of test mortars, BSI Standards Publication*
9. *BS EN 1015-3:(1999), Methods of Test for Masonry – Part 3: Determination of consistence of fresh mortar, BSI Standards Publication*
10. *Buhagiar, P. {1985). Structural masonry: experimental determination of the compressive strength of a wall, University of Malta.*

11. Bartolo, I. F. (1991). *The strength of the mortar joint : an investigation of the behaviour of the mortar joint under lateral loading in local unreinforced limestone masonry construction, University of Malta.*

12. Caldeira, F. E., Nalon, G. H., de Oliveira, D. S., Pedroti, L. G., Ribeiro, J. C. L., Ferreira, F. A., & Carvalho, J. M. F. (2020). *'Influence of joint thickness and strength of mortars on the compressive behaviour of prisms made of normal and high-strength concrete blocks', Construction and Building Materials, 234, 11741,* *https://doi.org/10.1016/j.conbuildmat.2019.117419*

13. Camilleri,J. (2023), *Kors Dwar Is-Sengha Tal-Bini, BDL Books.*

14. Caruana, L (2024), *'The Impact of Mortar Thickness on the Strength of Globigerina Limestone Masonry Wall', University of Malta.*

15. Drougkas, A., Roca, P. and Molins, C. (2015) *'Compressive strength and elasticity of pure lime mortar masonry', Materials and Structures, 49(3), pp. 983–999.* *https://doi.org/10.1617/s11527-015-0553-2*

16. EN 1996-1-1:(2005), *Eurocode 6: Design of Masonry Structures. General rules for reinforced and unreinforced masonry structures.*

17. Fonseca, F. S., Mohamad, G., Roman, H. R., Vermeltfoort, A. T., & Rizzatti, E. (2015). *'Deformation and failure mode of masonry'. In Proceedings of the 12th North American Masonry Conference (pp. 1–12). Denver, Colorado.*

18. Fonseca, F.,Mohamad, G., S., Vermeltfoort, A. T., Martens, D. R. W., & Lourenço, P. B. (2017). *'Strength, behaviour, and failure mode of hollow concrete masonry constructed with mortars of different strengths'. Construction & Building Materials, 134, 489–496* https://doi.org/10.1016/j.conbuildmat.2016.12.112

19. Glenn Zammit (2017). *The Characteristic Compressive Strength Of Masonry Walls With Reconstituted Limestone Blocks From Building Waste, University of Malta.*

20. Haach, V. G., Vasconcelos, G., & Lourenço, P. B. (2011). *Influence of aggregates grading and water/cement ratio in workability and hardened properties of mortars. Construction and Building Materials, 25(6), 2980–2987. https://doi.org/10.1016/j.conbuildmat.2010.11.011*

21. MSA EN 1996-3:(2006), *Eurocode 6: Design of Masonry Structures. Simplified calculation methods for unreinforced masonry structures.*

22. MCT Italy. (n.d.).(2025) *Ready mix batching plant in France. Retrieved June 9, 2025, from https://www.marcantonini.com/en/project/france/*

23. National Statistics Office Malta. (2021). *Regional Statistics MALTA 2020 Edition*

24. National Statistics Office Malta. (2022). *The state of the climate 2022: A multidecadal report and assessment of Malta's climate (Reference year 2020)*

25. Roberts, J. J., & Brooker, O. (2007). *How to design masonry structures using Eurocode 6, The Concrete Centre.*

26. Sarhat, S. R., & Sherwood, E. G. (2014). *The prediction of compressive strength of ungrouted hollow concrete block masonry. Construction and Building Materials, 58, 111–121.* https://doi.org/10.1016/j.conbuildmat.2014.01.025

27. Yancey, C. W. C., Fattal, S. G., & Dikkers, R. D. (1991). *Review of research literature on masonry shear walls (NIST IR 4512). National Institute of Standards and Technology. https://doi.org/10.6028/NIST.IR.4512*

Appendix A : Mortar Test Results

Prism number	Date cast	Date tested	Age	Dimensions			Load	Mpa
			days	length/mm	Breadth/mm	Height/mm	kN	Mpa
A1	10/12/2024	17/12/2024	7	160.87	40.28	40.09	1.495	3.5
A2	10/12/2024	17/12/2024	7	160.8	40.35	39.78	1.584	3.71
A3	10/12/2024	17/12/2024	7	160.82	40.72	40.85	1.507	3.53
Average							1.528666667	3.58
B1	10/12/2024	17/12/2024	7	161	40.32	40.24	0.225	0.53
B2	10/12/2024	17/12/2024	7	160.16	39.18	40.26	0.264	0.62
B3	10/12/2024	17/12/2024	7	160.3	40.89	40.14	0.269	0.63
Average							0.252666667	0.5933333
C1	10/12/2024	17/12/2024	7	160.63	40.4	40.22	0.743	1.74
C2	10/12/2024	17/12/2024	7	160.91	40	40	0.514	1.21
C3	10/12/2024	17/12/2024	7	160.52	40.05	39.5	0.65	1.52
Average							0.635666667	1.49

Prism number	Date cast	Date tested	Age	Load	Mpa
			days	kN	Mpa
A1.1	10/12/2024	17/12/2024	7	25.37	15.85
A1.2	10/12/2024	17/12/2024	7	25.97	16.23
A2.1	10/12/2024	17/12/2024	7	26.3	16.44
A2.2	10/12/2024	17/12/2024	7	25.8	16.12
A3.1	10/12/2024	17/12/2024	7	25.99	16.25
A3.2	10/12/2024	17/12/2024	7	19.31	12.07
Average				24.79	15.49333333
B1.1	10/12/2024	17/12/2024	7	2.48	1.55
B1.2	10/12/2024	17/12/2024	7	2.45	1.53
B2.1	10/12/2024	17/12/2024	7	3.14	1.96
B2.2	10/12/2024	17/12/2024	7	2.68	1.68
B3.1	10/12/2024	17/12/2024	7	2.85	1.68
B3.2	10/12/2024	17/12/2024	7	2.82	1.76
Average				2.736666667	1.693333333
C1.1	10/12/2024	17/12/2024	7	9.52	5.95
C1.2	10/12/2024	17/12/2024	7	6.99	4.37
C2.1	10/12/2024	17/12/2024	7	6.02	3.76
C2.2	10/12/2024	17/12/2024	7	6.08	3.8
C3.1	10/12/2024	17/12/2024	7	8.73	5.46
C3.2	10/12/2024	17/12/2024	7	9.03	5.64
Average				7.728333333	4.83

Table 6.1: 7-day Prism Flexural and Compressive Test

Prism number	Date cast	Date tested	Age	Dimensions			Load	Mpa
			days	*length/mm*	*Breadth/mm*	*Height/mm*	*kN*	*Mpa*
A1	10/12/2024	07/01/2025	28	160.27	39.97	40.49	2.675	6.27
A2	10/12/2024	07/01/2025	28	160.39	40.1	41.05	2.616	6.13
A3	10/12/2024	07/01/2025	28	160.34	40.06	40.89	2.694	6.31
Average							2.661666667	6.2366667
B1	10/12/2024	07/01/2025	28	161.42	40.73	39.96	0.349	0.82
B2	10/12/2024	07/01/2025	28	160.61	40.29	38.51	0.34	0.8
B3	10/12/2024	07/01/2025	28	159.9	39.95	39	0.379	0.89
Average							0.356	0.8366667
C1	10/12/2024	07/01/2025	28	160.93	39.36	40.3	0.946	2.22
C2	10/12/2024	07/01/2025	28	160.66	38.42	30.6	1.144	2.68
C3	10/12/2024	07/01/2025	28	160.23	39.15	40.1	1.326	3.11
Average							1.138666667	2.67

Prism number	Date cast	Date tested	Age	Load	Mpa
			days	*kN*	*Mpa*
A1.1	10/12/2024	07/01/2025	28	39.52	24.7
A1.2	10/12/2024	07/01/2025	28	39.01	24.38
A2.1	10/12/2024	07/01/2025	28	39.91	24.94
A2.2	10/12/2024	07/01/2025	28	41.01	25.63
A3.1	10/12/2024	07/01/2025	28	38.94	24.34
A3.2	10/12/2024	07/01/2025	28	40.1	25.06
Average				39.74833333	24.84166667
B1.1	10/12/2024	07/01/2025	28	3.75	2.35
B1.2	10/12/2024	07/01/2025	28	3.61	2.26
B2.1	10/12/2024	07/01/2025	28	3.79	2.37
B2.2	10/12/2024	07/01/2025	28	3.74	2.34
B3.1	10/12/2024	07/01/2025	28	4.68	2.92
B3.2	10/12/2024	07/01/2025	28	4.63	2.89
Average				4.033333333	2.521666667
C1.1	10/12/2024	07/01/2025	28	11.11	6.95
C1.2	10/12/2024	07/01/2025	28	11.3	7.06
C2.1	10/12/2024	07/01/2025	28	10.45	6.53
C2.2	10/12/2024	07/01/2025	28	11.43	7.14
C3.1	10/12/2024	07/01/2025	28	15.48	9.68
C3.2	10/12/2024	07/01/2025	28	16.01	10.01
Average				12.63	7.895

Table 6.2: 28-day Prism Flexural and Compressive Test

Cube number	Date cast	Date tested	Age	Load	Mpa
			days	*kN*	*Mpa*
A4	09/05/2025	12/05/2025	3	28.97	11.59
A5	09/05/2025	12/05/2025	3	33.95	13.58
A6	13/05/2025	16/05/2025	3	18.19	7.28
A7	13/05/2025	16/05/2025	3	27.89	11.16
A8	13/05/2025	16/05/2025	3	27.51	11
A9	13/05/2025	16/05/2025	3	22.11	8.84
A10	16/05/2025	19/05/2025	3	16.46	6.58
A11	16/05/2025	19/05/2025	3	13.59	5.43
A12	20/05/2025	23/05/2025	3	33.33	13.33
A13	20/05/2025	23/05/2025	3	35.42	14.17
A14	20/05/2025	23/05/2025	3	25.44	10.18
A15	20/05/2025	23/05/2025	3	40.23	16.09
A16	20/05/2025	23/05/2025	3	39.66	15.86
A17	20/05/2025	23/05/2025	3	38.9	15.56
A18	20/05/2025	23/05/2025	3	41.73	16.69
A19	20/05/2025	23/05/2025	3	40.81	16.32
A20	20/05/2025	23/05/2025	3	35.15	14.06
Average				30.54941176	12.21882353

Table 6.3: 3-day Cube Compressive Test Results

Flexural Tests of MIX A, MIX B, MIX C

The plot shows the results observed of all 3 mixes of both the 7 day and 28-day test results. The mean 7-day test results for the flexural strength of the M6, Xaħx, M2 mixes were 3.58 MPa, 0.59 MPa and 1.49 MPa, respectively. The mean 28-day test results for the flexural strength of the M6, Xaħx, M2 mixes were 6.24 MPa, 0.84 MPa and 2.67 MPa, respectively.

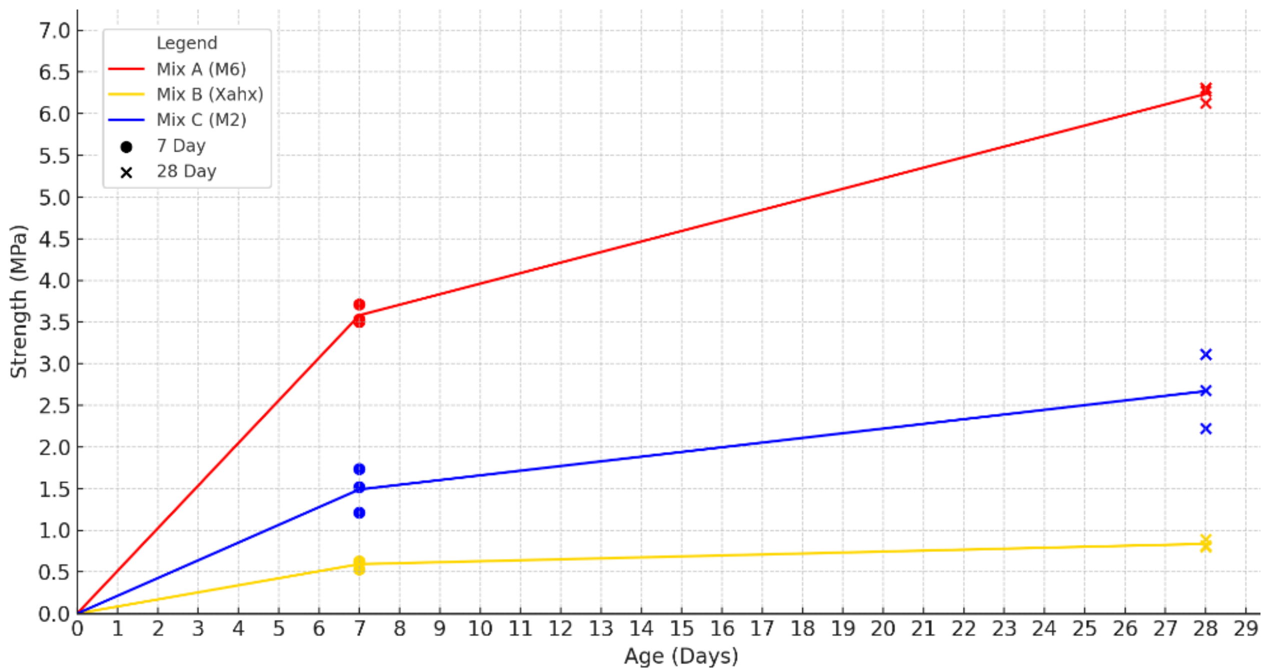

Figure 6.1: Plot of Flexural Strength Test Results of Mix A,B and C

(28-Day)

(7- Day)

Figure 6.2 Images of 28 and 7 Day Three Point Flexural Test